

2023/07/19

9:30-10:00

Moonshot Goal 6: International Symposium 2023



Progress reports on
**Development of Integration Technologies for
Superconducting Quantum Circuits**

Secure System Platform Research Laboratories

NEC Corporation

Tsuyoshi Yamamoto

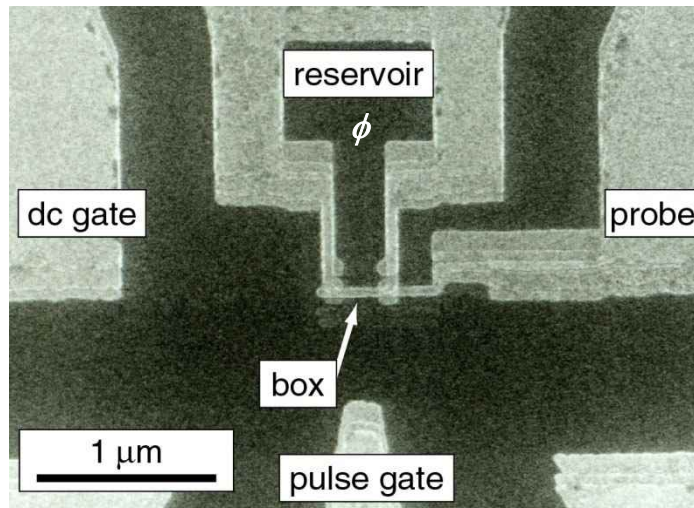
<https://ms-iscqc.jp/en/>

Table of contents

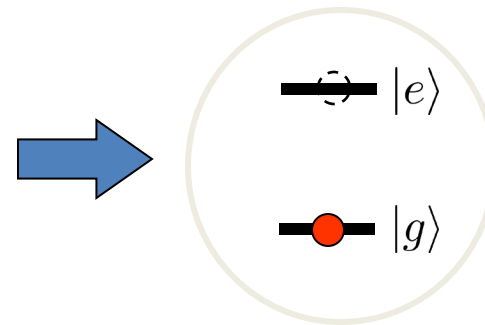
1. Introduction of the project
2. Progress report
 - Overview
 - Demonstration of Kerr cat qubit
 - SIS-mixer-based microwave amplifier
3. Plans for the second half of the project

Superconducting qubit

- ◆ electric circuit made of superconductor and Josephson junctions
- ◆ nonlinear oscillator with ~ 5 GHz resonance frequency
- ◆ operated at ~ 10 mK using a dilution refrigerator
- ◆ lithographically fabricated (\Leftrightarrow decoherence)
- ◆ design flexibility (\Leftrightarrow non uniformity)



Y. Nakamura et al., Nature **398**, 786 (1999).



Superconducting NISQ processors

Google
Article

Arute *et al.*, Nature **574**, 505 (2019).

Quantum supremacy using a programmable superconducting processor

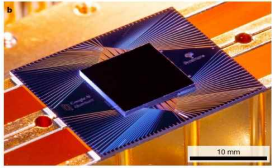
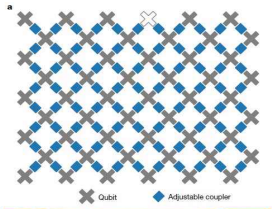
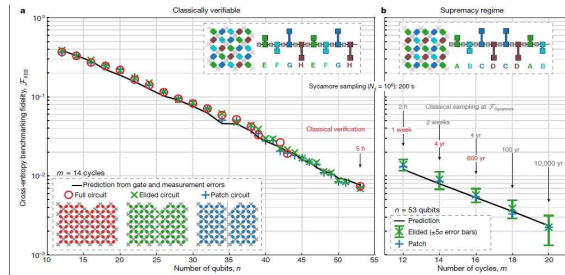
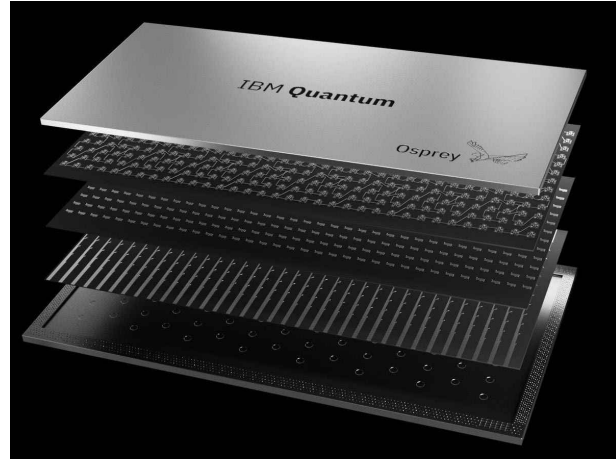


Fig. 1 The Sycamore processor. a, Layout of processor, showing a rectangular array of 54 qubits (grey), each connected to its four nearest neighbours with complex couplers. The inoperable qubit is outlined. b, Photograph of the Sycamore chip.



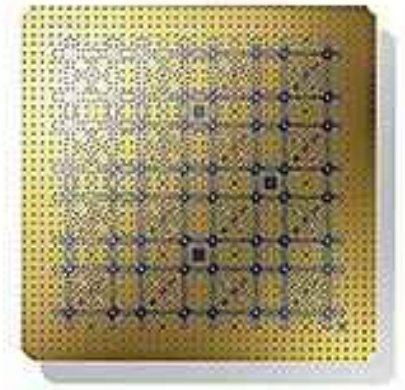
In reaching this milestone, we show that quantum speedup is achievable in a real-world system and is not precluded by any hidden physical laws. Quantum supremacy also heralds the era of noisy intermediate-scale quantum (NISQ) technologies¹⁵. The benchmark task we demon-

IBM, 433 qubits



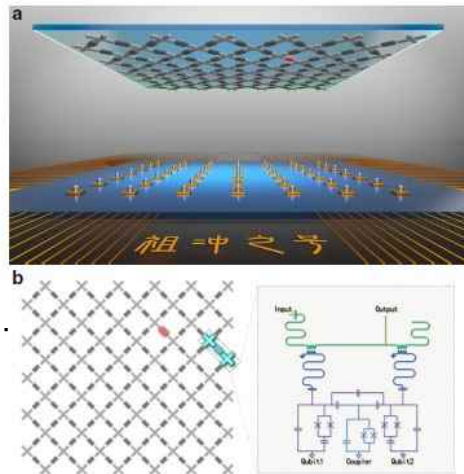
[IBM Unveils 433-Qubit Osprey Chip - IEEE Spectrum](#)

RIKEN RQC, 64 qubits



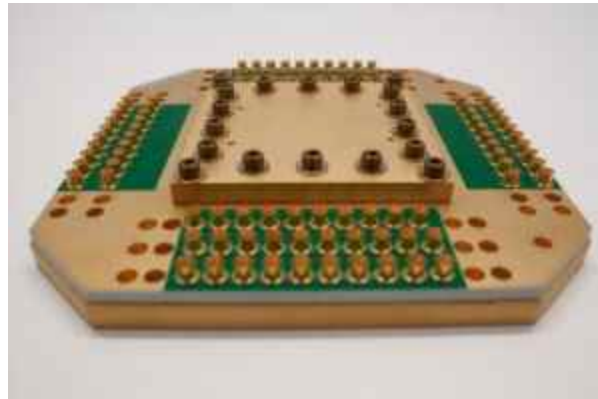
[理化学研究所量子コンピュータ研究センターセンター長 中村泰信氏 | 電子デバイス産業新聞 \(旧半導体産業新聞\) \(sangyo-times.jp\)](#)

USTC, 66 qubits



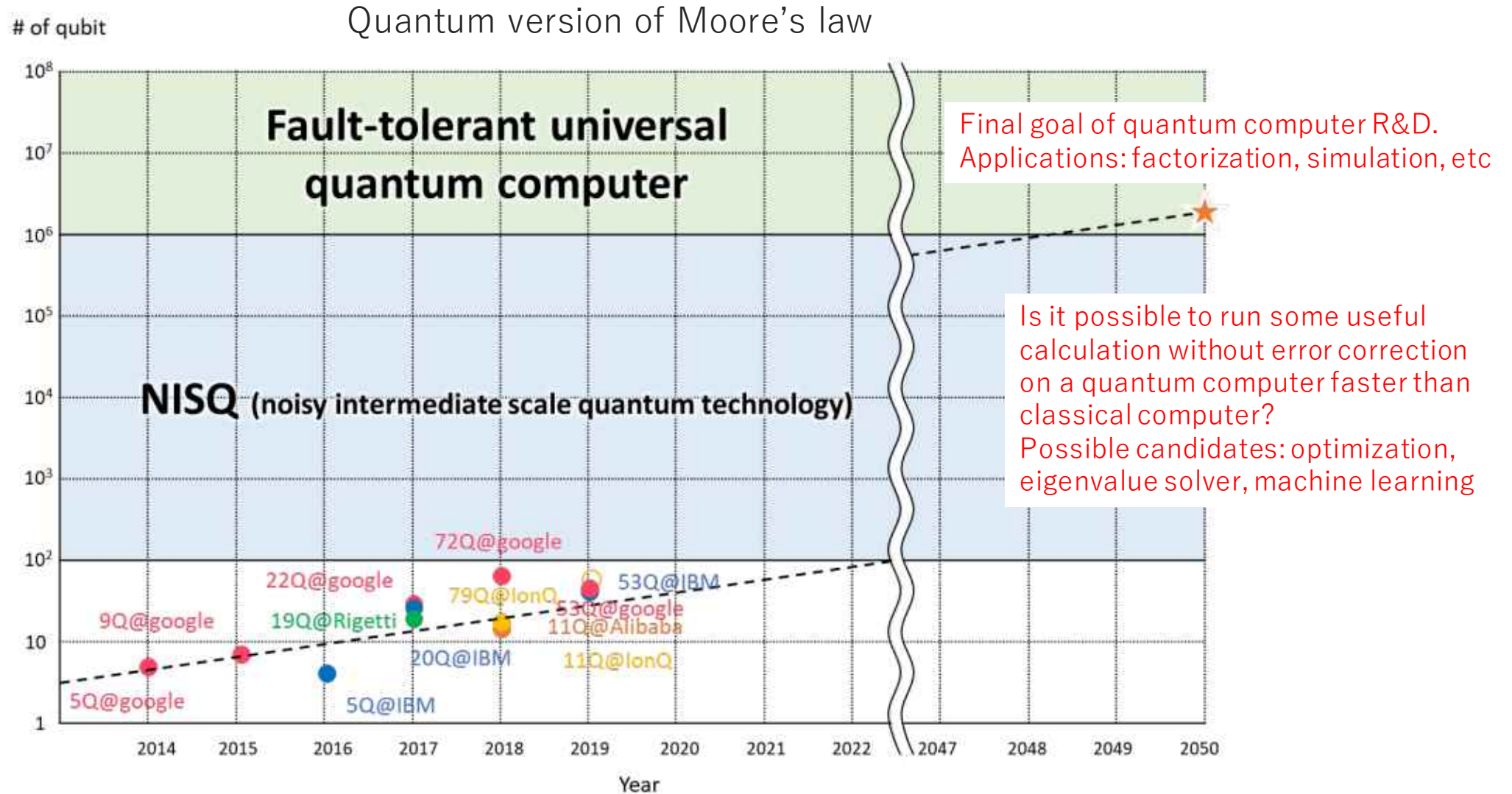
Zhu *et al.*,
Science Bulletin **67**, 240 (2022).

Rigetti, 80 qubits



[Rigetti Announces Commercial Availability of Aspen-M System and Results of CLOPS Speed Tests \(hpcwire.com\)](#)

beyond NISQ



Toward realization of fault-tolerant QC

◆ Two main problems in hardware development:

- required large number of physical qubits

Physical qubit error rate	10^{-3}	10^{-6}	10^{-9}
Physical qubits per logical qubit	15,313	1,103	313
Total physical qubits in processor	1.7×10^6	1.1×10^5	3.5×10^4
Number of T state factories	202	68	38
Number of physical qubits per factory	8.7×10^5	1.7×10^4	5.0×10^3
Total number of physical qubits including T state factories	1.8×10^8	1.3×10^6	2.3×10^5

~ 10^8 qubits?

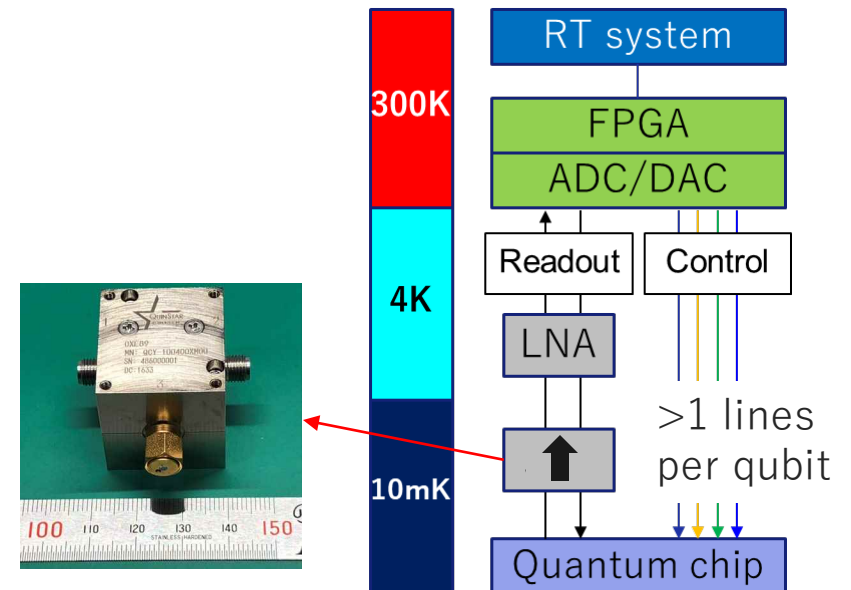
- not scalable wiring & electronics

- >1 coax line per qubit from RT to mK for control
- bulky μ -wave components (amplifier, isolator) for readout

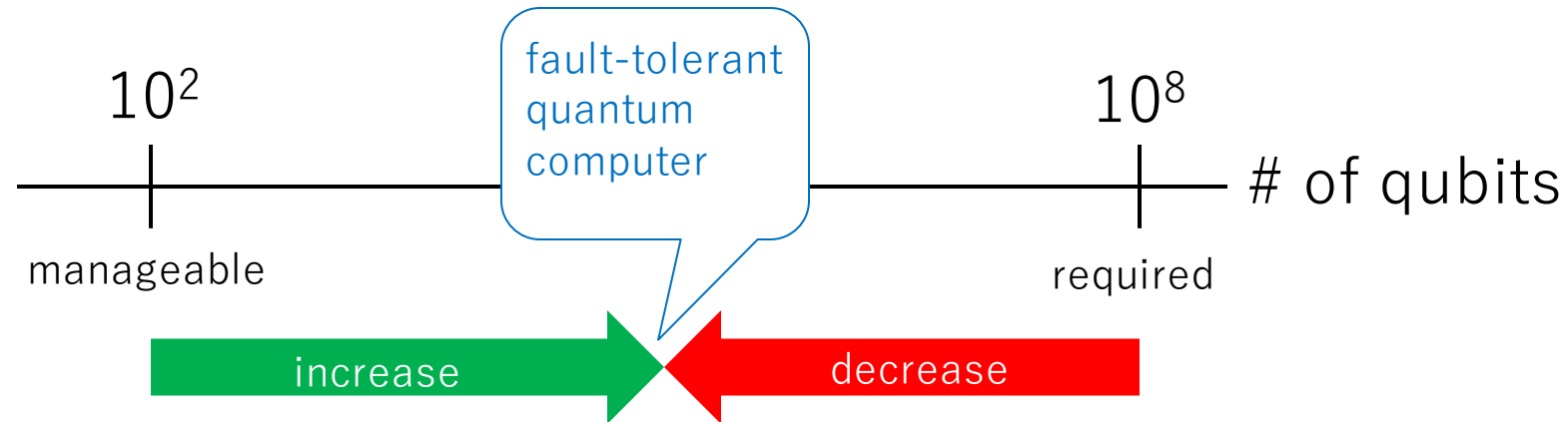
<~ 10^2 qubits?

TABLE 3.1 Estimates of the Resource Requirements for Carrying Out Error-Corrected Simulations of a Chemical Structure (FeMoco in Nitrogenase) Using a Serial Algorithmic Approach for Hamiltonian Simulation and the Surface Code for Error Correction

Quantum Computing: Progress and Prospects (2019)



Required technologies



System-level architecture optimization

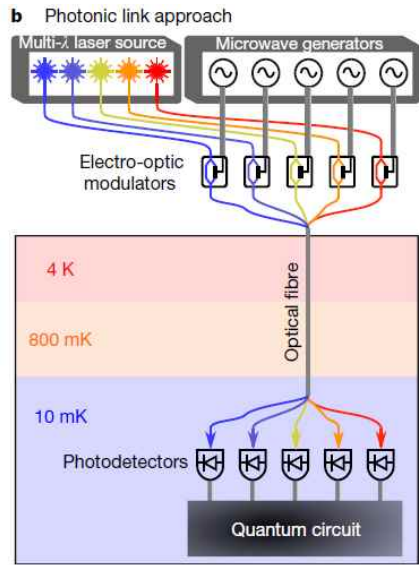
- cryo-electronics
- high-cooling-power refrigerator
- high-density wiring
- chip-to-chip interconnection
- ...
- improved coherence
- gate optimization
- hardware-efficient QEC scheme
- ...

Complex scalability trade-offs with huge design-parameter space
e.g. power consumption vs. logical error rate

I. Byun et al., Proceedings of the 49th Annual International Symposium on Computer Architecture, 366 (2022).

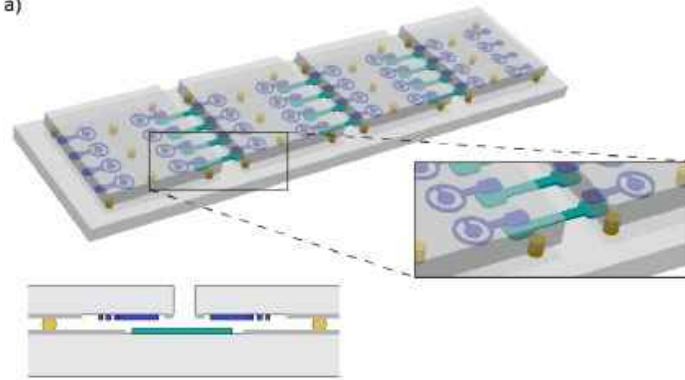
Beyond brute force approach

qubit control via optical fiber (NIST)



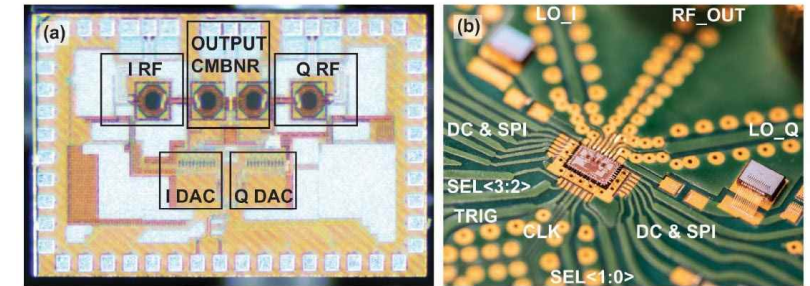
F. Lecocq et al., Nature **591**, 575 (2021).

inter-chip connection (Rigetti)



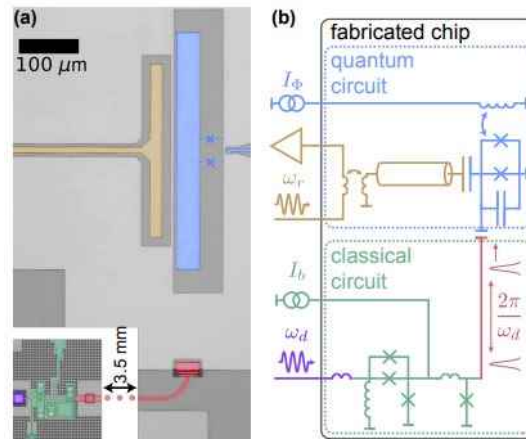
A. Gold et al., NPJ Quant. Inf. **7**, 142 (2021).

cryo-CMOS (Google)



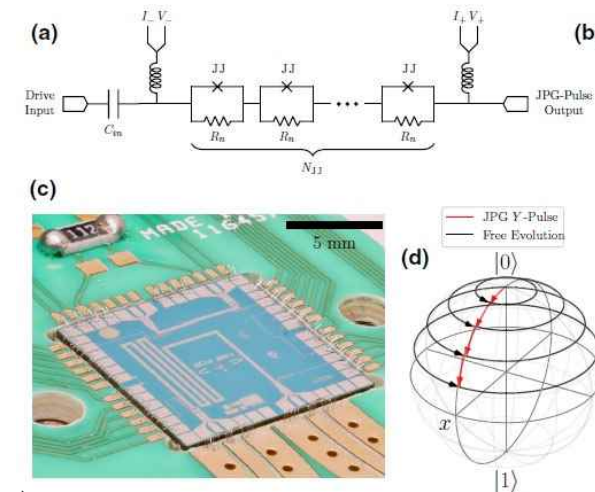
J. C. Bardin et al., IEEE J. Solid-State Circuits **54**, 3043 (2019).

qubit control using SFQ pulse (Wisconsin/Syracuse)



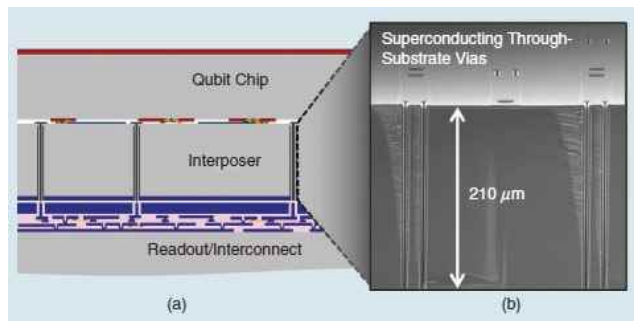
E. Leonard Jr. et al., Phys. Rev. Applied **11**, 014009 (2019).

qubit control using Josephson pulse generator (NIST)



L. Howe et al., PRX Quant. **3**, 010350 (2022).

stacked chip structure (MIT)



D. Rosenberg et al., IEEE Microw. Mag. **21**, 72 (2020).

Architecture for superconducting quantum computer system

On-line quantum error correction using SFQ decoder

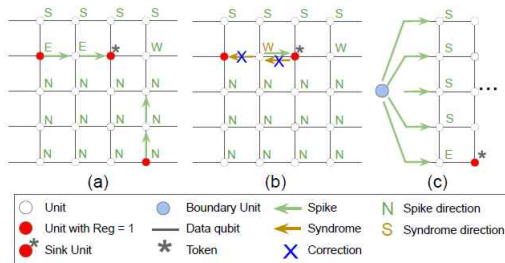


Fig. 2. Overview of the processing of our algorithm.

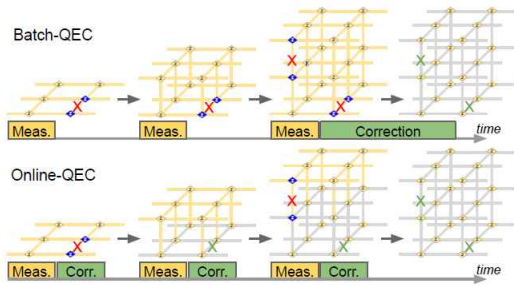


Fig. 3. Concept of Batch- and Online-QEC

the Univ. of Tokyo
Y. Ueno et al., 2021 58th ACM/IEEE Design Automation Conference (DAC), pp. 451-456

Scalable qubit control system using SFQ circuits

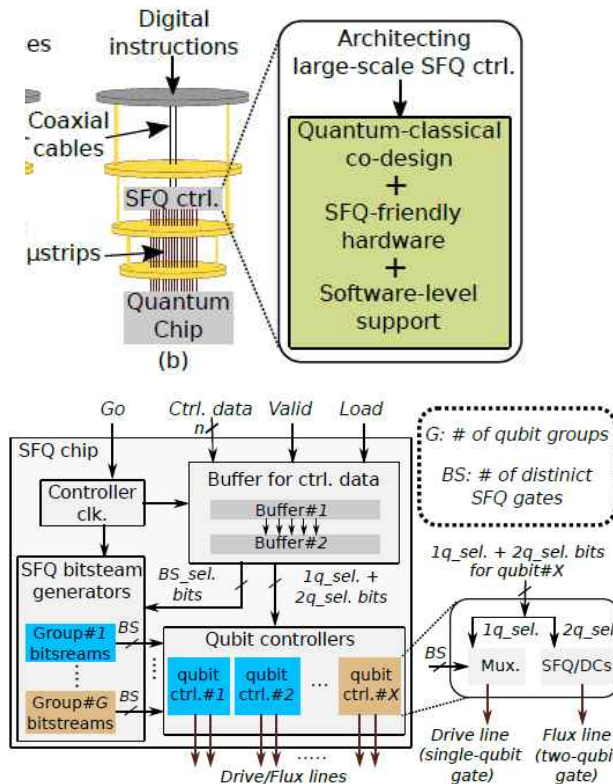
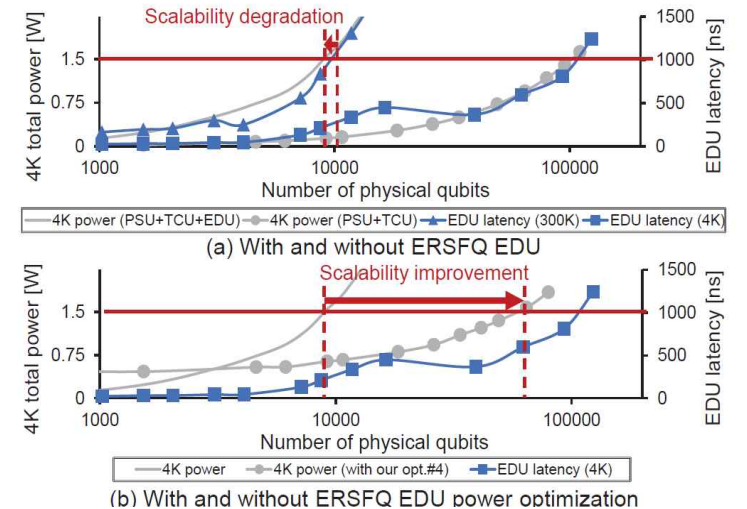
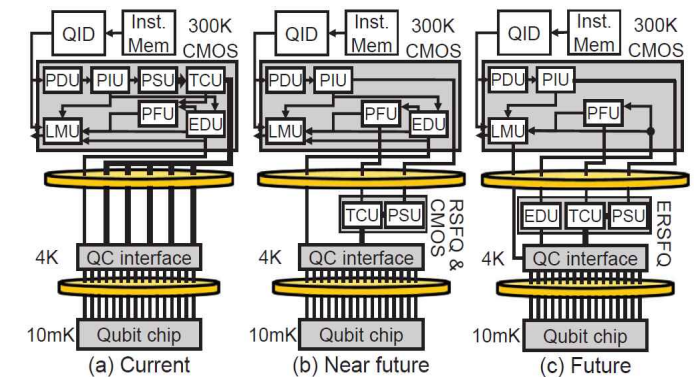


Figure 5: Overview of our *DigiQ* architecture.

Univ. of Chicago
M. R. Jokar et al., arXiv:2202.01407.

Optimization of error correction micro architecture using Cryo-CMOS and SFQ circuits



Seoul Univ.
I. Byun et al., Proceedings of the 49th Annual International Symposium on Computer Architecture, 366 (2022).

Project teams

6 private companies, 8 universities, 4 national institutes

R&D Target 1: high-quality superconducting qubit for FTQC

qubit decoherence, fabrication with multilayer process, magnetic junctions, bosonic qubits



R&D Target 2: hardware system for integrated superconducting qubits

refrigerator, packaging, cryogenic amplifiers



ULVAC CRYOGENICS INC.



R&D Target 3: scalable electronics for quantum error correction

RT electronics, cryo-electronics (superconducting flux quantum circuits, cryoFPGA, cryoCMOS), QC architecture



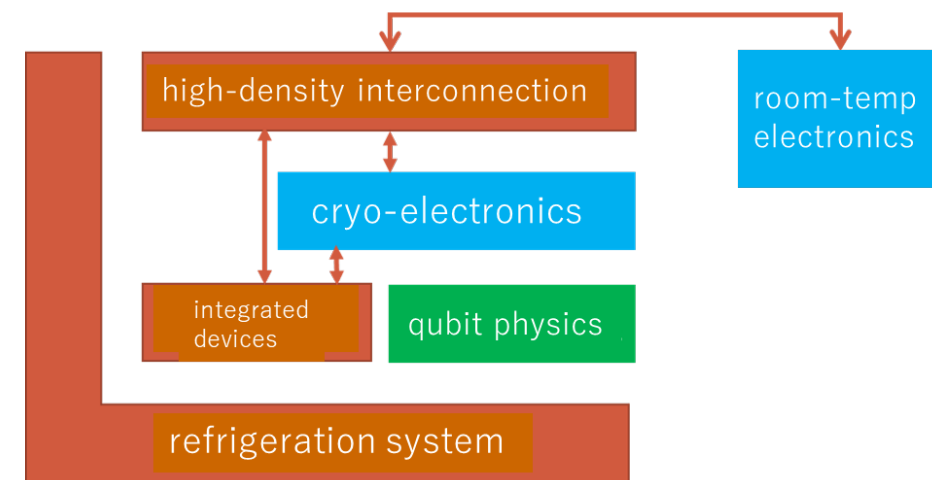
NAGOYA UNIVERSITY



OSAKA UNIVERSITY



KYUSHU UNIVERSITY



Research themes and PI's

R&D Target 1: high-quality superconducting qubit for FTQC
 R&D Target 2: hardware system for integrated superconducting qubits
 R&D Target 3: scalable electronics for quantum error correction

M. Negoro



K. Inoue



Kyushu Univ : system design for superconducting FTQC

Y. Uzawa



A. Kawakami



NAOJ, NICT: SIS-mixer-based microwave amplifier

300K Room temperature system

Osaka Univ. : Scalable Electronics for Quantum Computers

M. Tada K. Uchida



NBS, Univ. of Tokyo : cryo FPGA

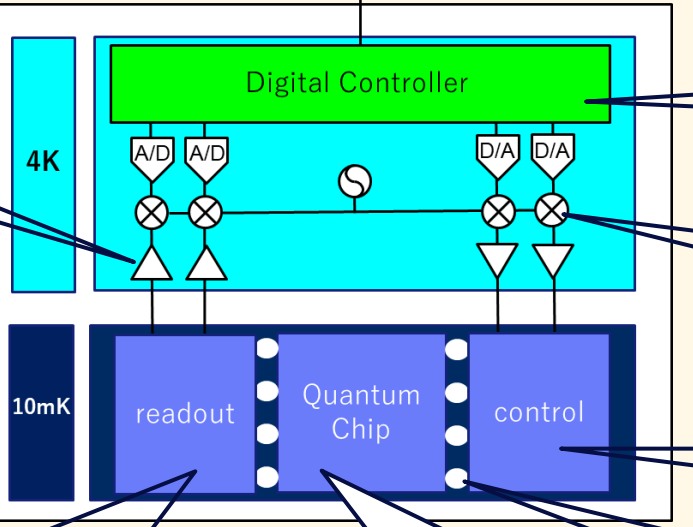
M. Saito



Y. Fujiwara



ULVAC, ULVAC Cryogenics : Refrigeration Systems for Quantum Computing



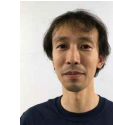
Keio Univ., Univ. of Tokyo: high-frequency analog circuits for low temperature operation

H. Ishikuro



Nagoya Univ., NEC: Qubit control using a single flux quantum circuit

M. Tanaka T. Yamamoto



K. Koshino



Nagoya Univ., TMDU, RIKEN, NEC: Qubit readout using a single flux quantum circuit

S. Yorozu



RIKEN: Stacked structure of chips with different functions

NEC, AIST: Improvement of qubit lifetime and coherence
 Tokyo Medical and Dental University: Theoretical study on the qubit readout
 NICT, Tohoku Univ.: Qubit with epitaxial junction and magnetic junction
 NIKON: Qubit fabrication using CMOS compatible process
 NTT, Tokyo University of Science, RIKEN: Bosonic code using superconducting circuits

K. Inomata



F. Yoshihara



S. Saito



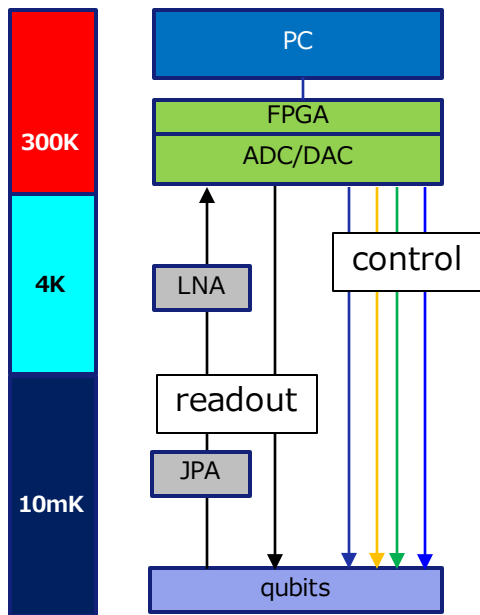
J. S. Tsai



Goals of the project

start of the project

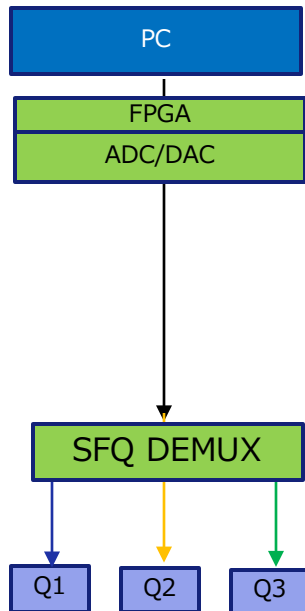
2020



Control and readout with RT electronics
Coax cables $> 1/\text{qubit}$

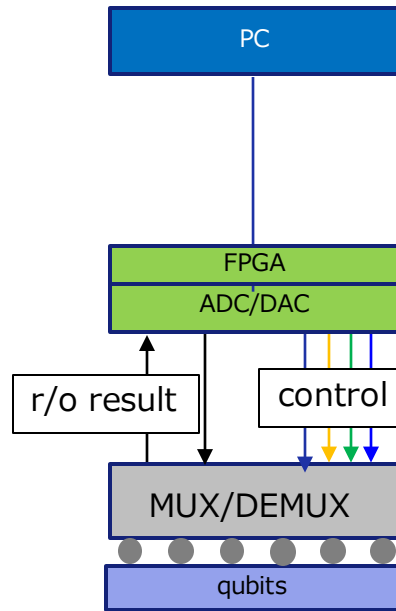
Goal of current project

2025



Evaluation of individual components
e.g. SFQ demultiplexer (figure), SIS-mixer based amplifier, etc

2030

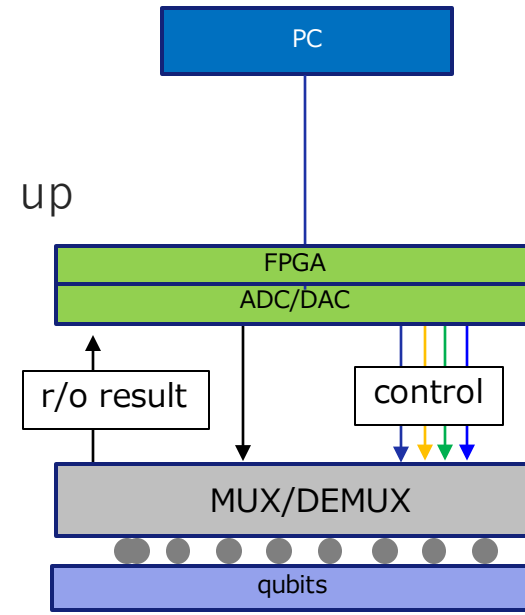


Error correction with cryo-electronics
Coax cables $< 1/\text{qubit}$

strategy for further scale up



2040



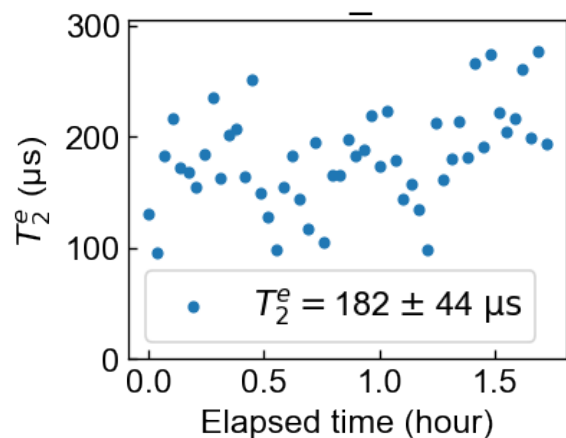
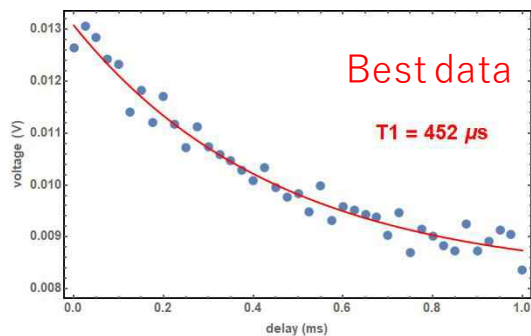
Research progress

Research highlights (Target 1: high-quality superconducting qubit for FTQC)

details later

RIKEN + NICT teams

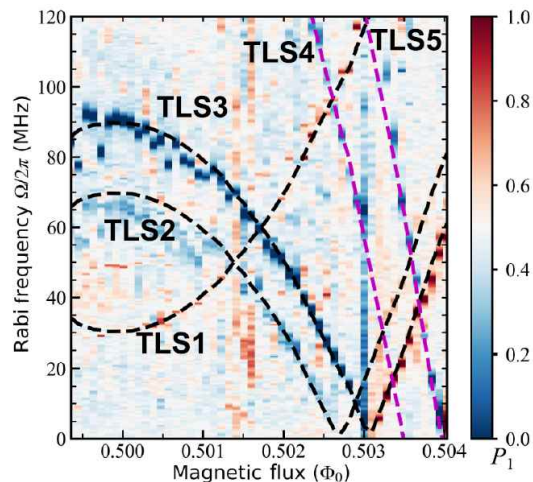
High-performance transmon qubits with an epitaxially grown TiN film



A. Noguchi et al.,
APS March Meeting 2023, M73-5

NTT team

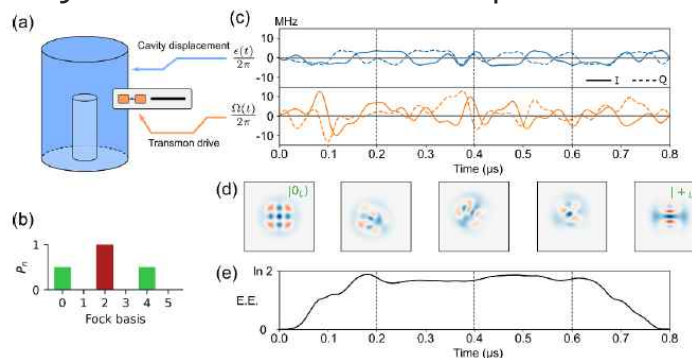
Identification of different types of TLS defects



L. V. Abdurakhimov et al., PRX Quantum **3**, 040332 (2022).

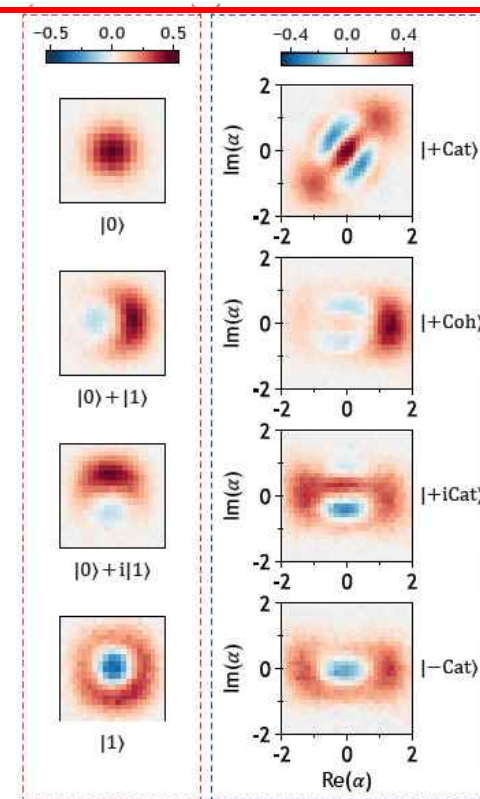
Gate error analysis in SC bosonic qubit

K. Mizuno et al.,
New J. Phys. **25**
(2023) 033007.



Tokyo university of science team

Wigner tomography and gate operations of Kerr cat qubit



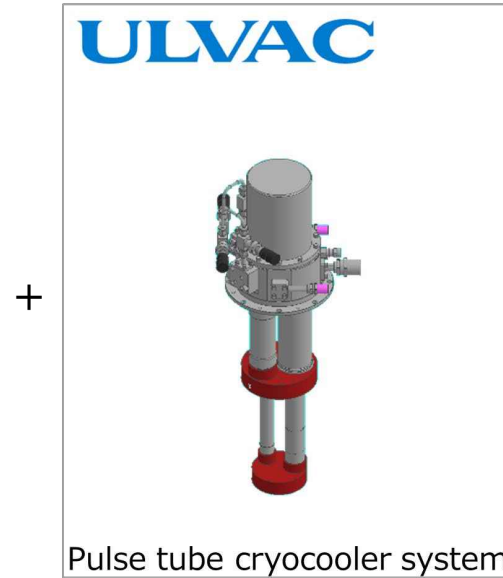
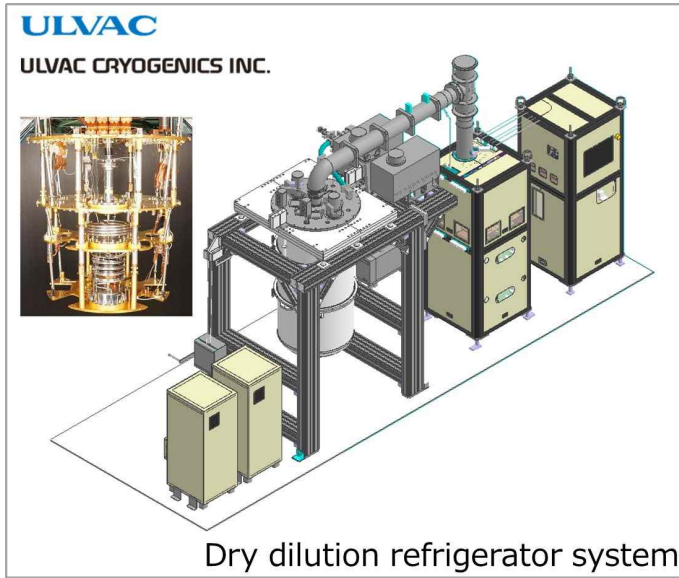
Iyama et al., arXiv:2306.12299.

S. Kwon et al., NPJ Quantum Inf. **8**, 40 (2022).

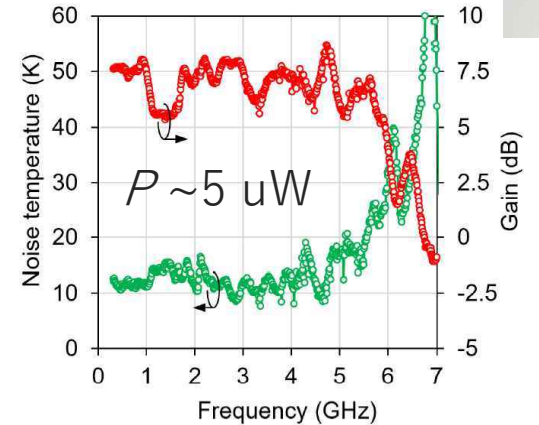
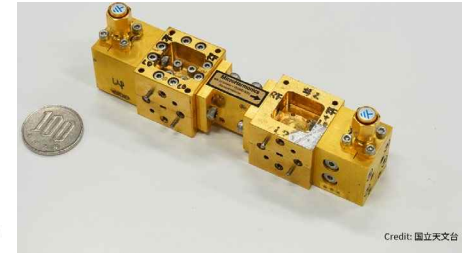
Research highlights (Target 2: hardware system for integrated superconducting qubits)

details later

Refrigeration system for quantum computing

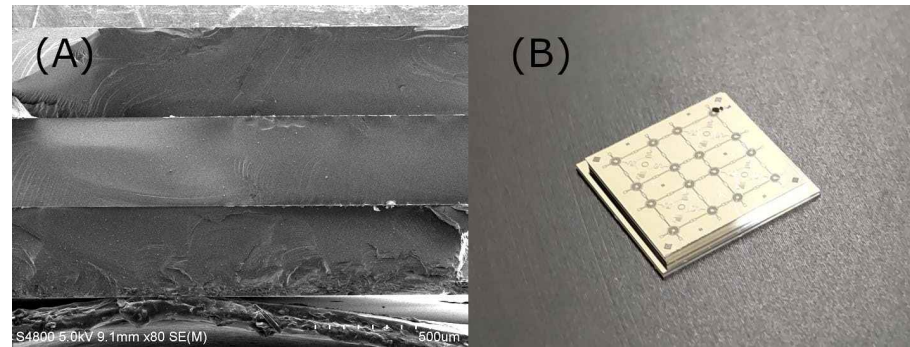
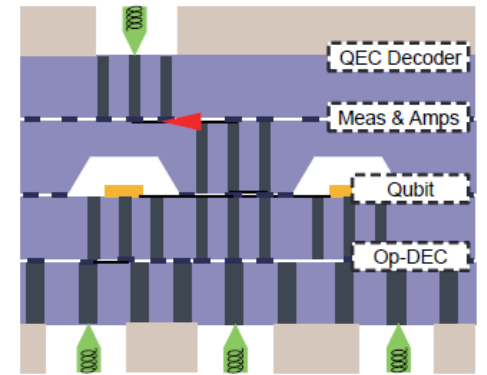


NAOJ + NICT teams
SIS-mixer-based microwave amplifier



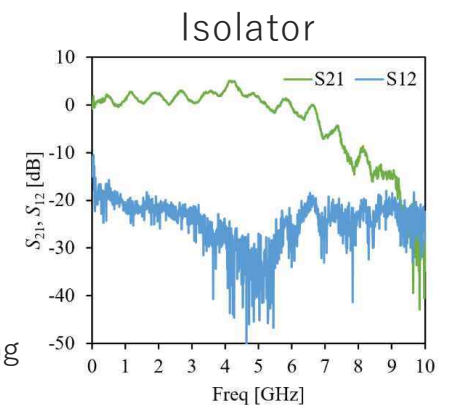
T. Kojima et al.,
Appl. Phys. Lett. **122**,
072601 (2023).

RIKEN team



3-tier stack test device
(A) cross-section (B) exterior

S. Masui et al.,
JSAP meeting 2023 spring

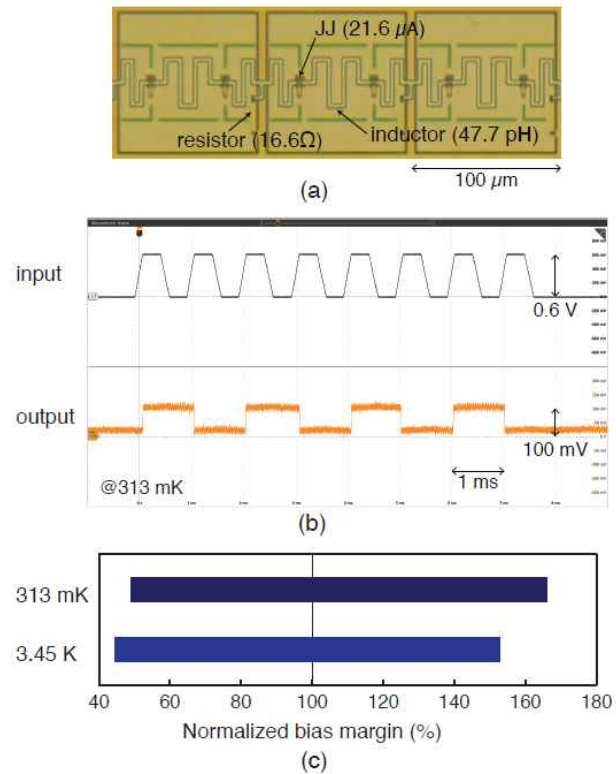


Y. Tabuchi et al.,
2021 Symposium on VLSI Technology, pp. 1-2.

Research highlights (Target 3: scalable electronics for quantum error correction)

Nagoya Univ. + NEC teams

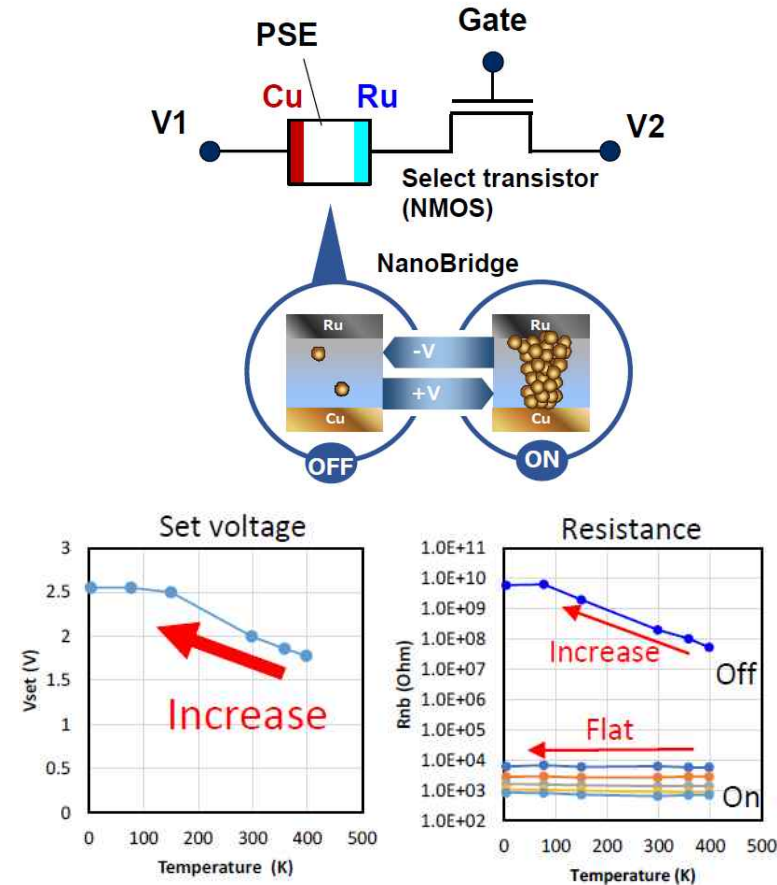
Design and operation of low-power SFQ circuits ($j_c=255 \text{ A/cm}^2$, $P=7.5 \text{ nW/JJ}$)



M. Tanaka et al., IEEE Trans. Appl. Supercond. **33**, 1700805 (2023).

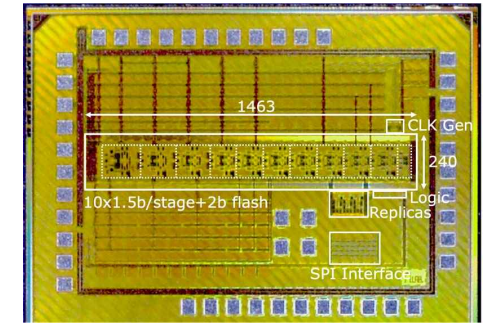
NBS + Keio Univ. + Univ. of Tokyo teams

Cryogenic operation of NanoBridge

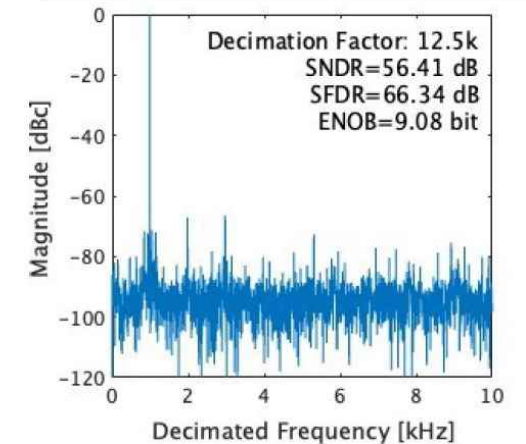


K. Okamoto et al., Jpn. J. Appl. Phys. **61**, SC1049 (2022).

Cryo-ADC prototype device



Measured Spectra at 4.6K with 125MHz input

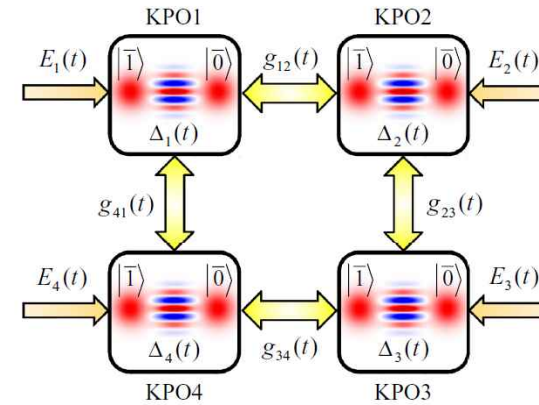


K. Yamashita et al., IEEE Custom Integrated Circuit Conference (CICC 2023).

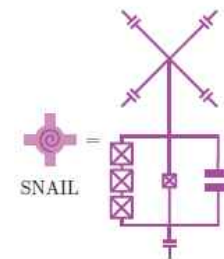
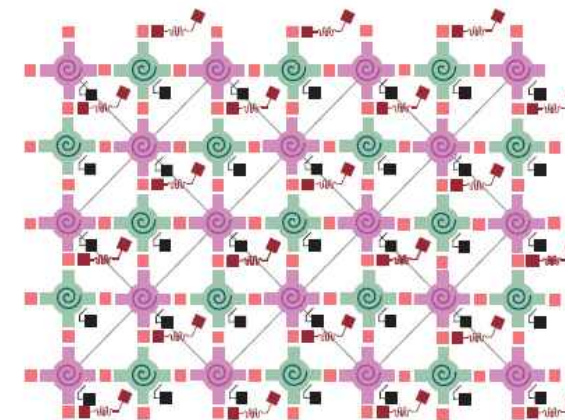
Wigner tomography and gate operations of Kerr cat qubit

Hardware-efficient FTQC using Kerr cat qubit

- ◆ Theory of Kerr cat qubit
 - P. T. Cochrane et al., Phys. Rev. A **59**, 2631 (1999).
 - H. Goto, Phys. Rev. A **93**, 050301 (2016).
 - S. Puri et al., npj Quantum Info. **3**, 18 (2017).
- ◆ High-fidelity gate operation
 - T. Kanao et al., Phys. Rev. Appl. **18**, 014019 (2022).
 - H. Chono et al., Phys. Rev. Res. **4**, 043054 (2022).
- ◆ Proposal of bias preserving gate
 - S. Puri et al., Sci. Adv. **6**, eaay5901 (2020).
- ◆ Error-correction code with high error threshold
 - A. S. Darmawan et al., PRX Quantum **2**, 030345 (2021).
- ◆ Experiments
 - Z. Wang et al., Phys. Rev. X **9**, 021049 (2019).
 - A. Grimm et al., Nature **584**, 205 (2020).
 - N. E. Frattini et al., arXiv:2209.03934.
 - J. Venkatraman et al., arXiv:2211.04605.



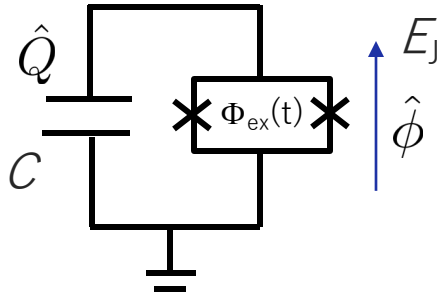
Goto, PRA 2016



- ◆ = de flux bias for the SNAIL
- ◆ = resonator for qubit readout
- = out-of-plane interconnect through which all the microwave drives (such as the two-photon drives, coupling drives for CX gates and drives for single-qubit gates) are applied

Darmawan et al., PRX Quantum 2021

Hamiltonian of KPO



$$\mathcal{H}_{\text{KPO}} = \hbar\omega_0 \left(a^\dagger a + \frac{1}{2} \right) - \frac{E_c}{12} (a^\dagger + a)^4 + \frac{\hbar\omega_0}{4} \frac{\delta E_J}{E_J} (a^\dagger + a)^2 \cos \omega_p t$$



rotating frame at $\omega_p/2$, and RWA

$$\mathcal{H}_{\text{KPO}}' / \hbar = \Delta a^\dagger a - \frac{K}{2} a^\dagger a^\dagger a a + \frac{\beta}{2} (a^{\dagger 2} + a^2)$$

detuning Kerr nonlinearity parametric drive

$$\Delta = \omega_0 - K - \omega_p/2$$

$$K = E_c$$

$$\beta = \frac{\omega_0}{4} \frac{\delta E_J}{E_J}$$

$$E_J(t) = E_J + \delta E_J \cos \omega_p t$$

$$\hat{\phi} = \left(\frac{2E_c}{E_J} \right)^{1/4} (a^\dagger + a)$$

$$\hat{Q} = i \left(\frac{E_J}{2E_c} \right)^{1/4} (a^\dagger - a)$$

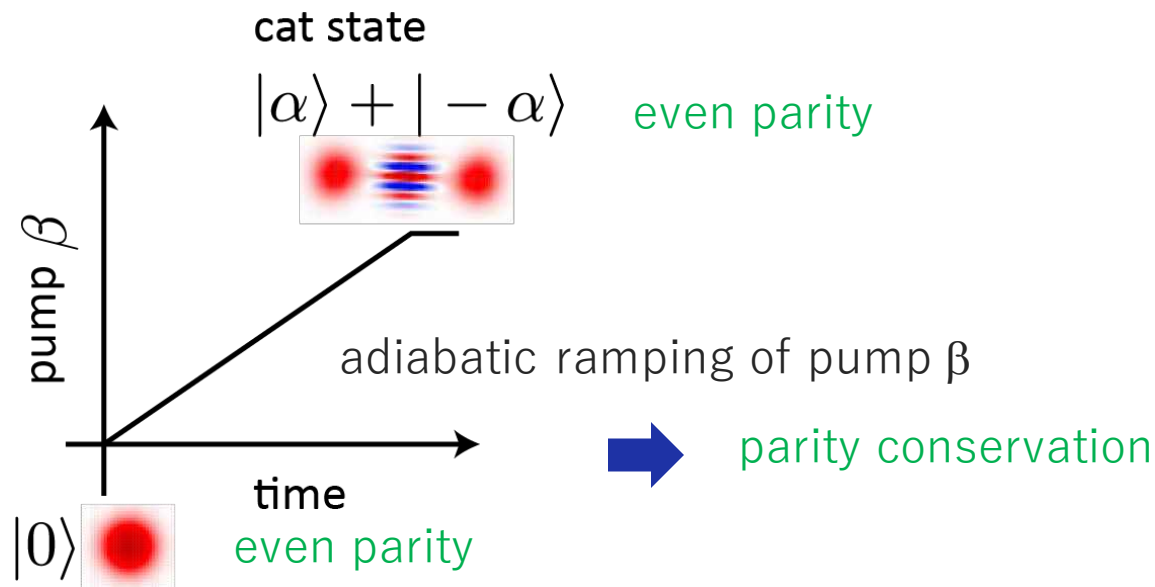
Generation of Schrodinger's cat state

$$\begin{aligned} \mathcal{H}_{\text{KPO}}/\hbar &= -\frac{K}{2}a^\dagger a^\dagger a a + \frac{\beta}{2}(a^{\dagger 2} + a^2) \\ &= -K\left(a^{\dagger 2} - \frac{\beta}{K}\right)\left(a^2 - \frac{\beta}{K}\right) + \frac{\beta^2}{K} \end{aligned}$$

P. T. Cochrane et al., Phys. Rev. A **59**, 2631 (1999).
 H. Goto, Sci. Rep. **6**, 21686 (2016).
 S. Puri et al., npj Quantum Info. **3**, 18 (2017).

Coherent state is an eigenstate of annihilation operator a , $a|\alpha\rangle = \alpha|\alpha\rangle$

H_{KPO} has degenerate eigenstates of $|\pm\alpha\rangle$, where $\alpha = \sqrt{\frac{\beta}{K}}$



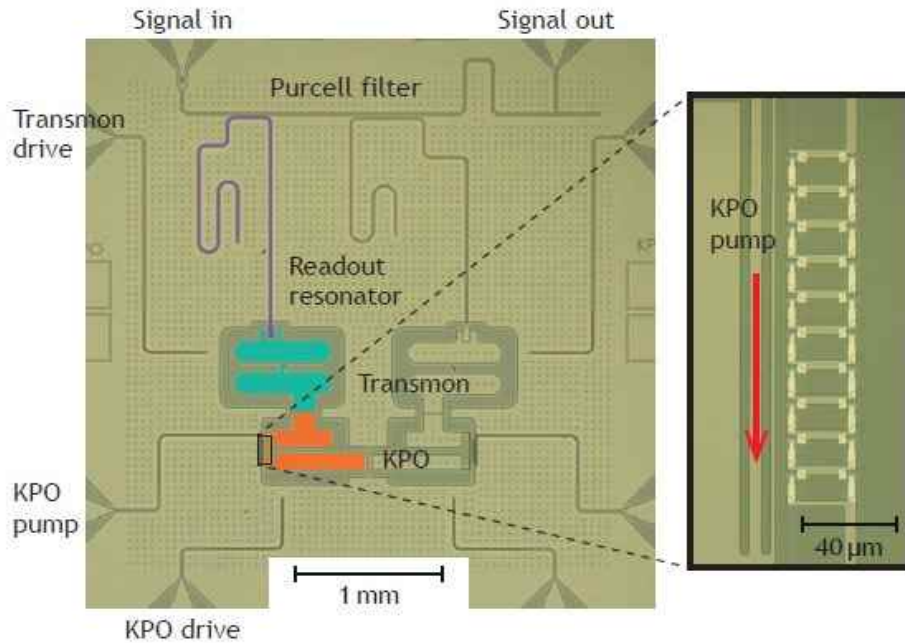
Generation of Kerr cat qubit

J. S. Tsai



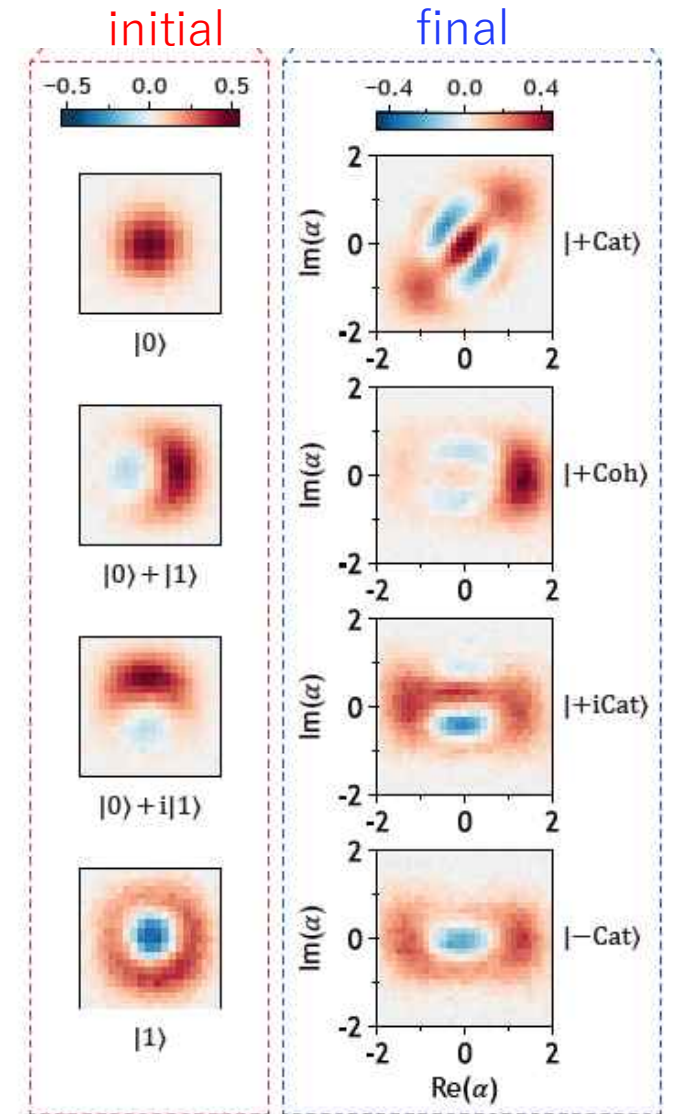
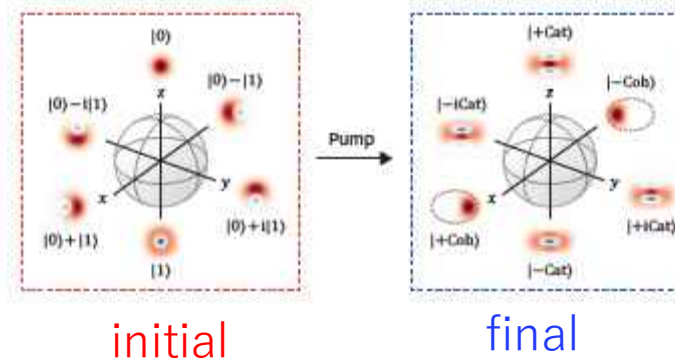
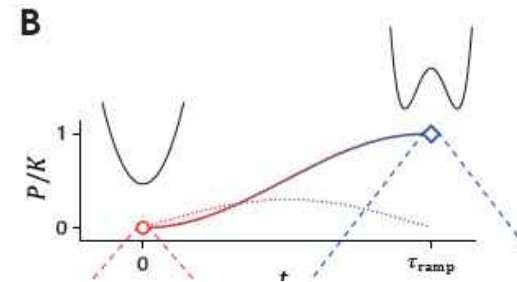
Wigner tomography

Device picture (coupled KPO device)



Iyama et al., arXiv:2306.12299.

adiabatic pumping
(with counter diabatic pump)



c.f.
Z. Wang et al., Phys. Rev. X **9**, 021049 (2019).
A. Grimm *et al.*, Nature **584**, 205 (2020).

R_x gate

P. T. Cochrane et al., Phys. Rev. A **59**, 2631 (1999).
 H. Goto, Sci. Rep. **6**, 21686 (2016).
 S. Puri et al., npj Quantum Info. **3**, 18 (2017).

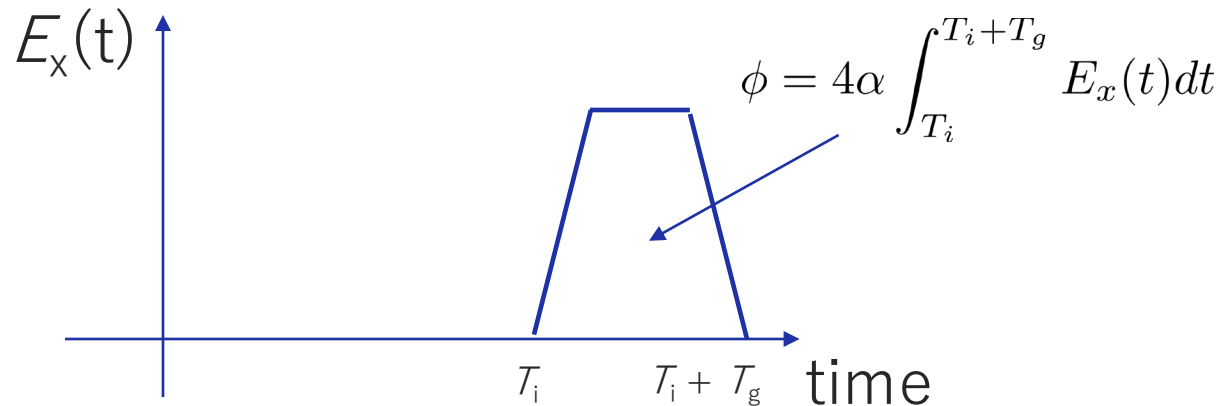
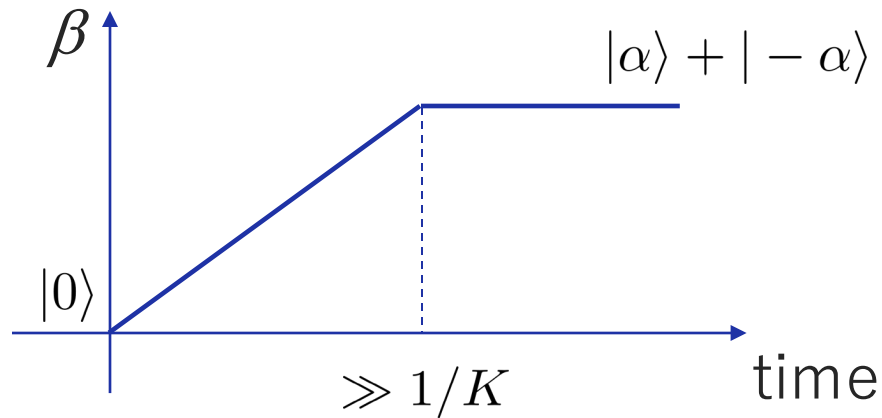
single-photon drive @ $\omega_p/2$

$$\mathcal{H}_{\text{KPO}}/\hbar = -\frac{K}{2}a^\dagger a^\dagger a a + \beta(a^{\dagger 2} + a^2) + E_x(t)(a + a^\dagger)$$

produces energy difference between $|\alpha\rangle$ and $|\alpha\rangle$

$$\langle \alpha | E_x(t)(a + a^\dagger) | \alpha \rangle = 2\alpha E_x(t)$$

$$\langle -\alpha | E_x(t)(a + a^\dagger) | -\alpha \rangle = -2\alpha E_x(t)$$



in α basis

change to cat basis

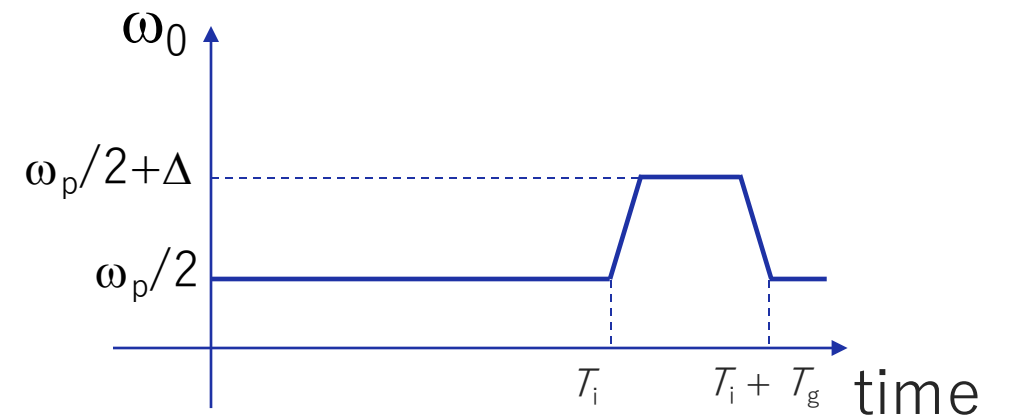
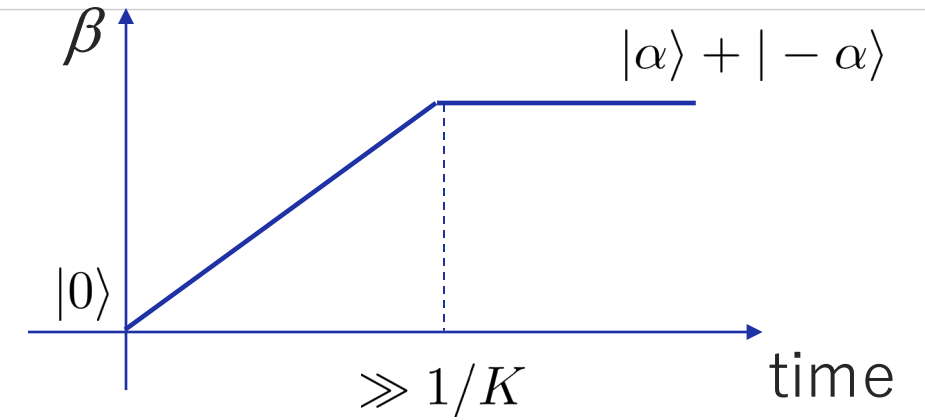
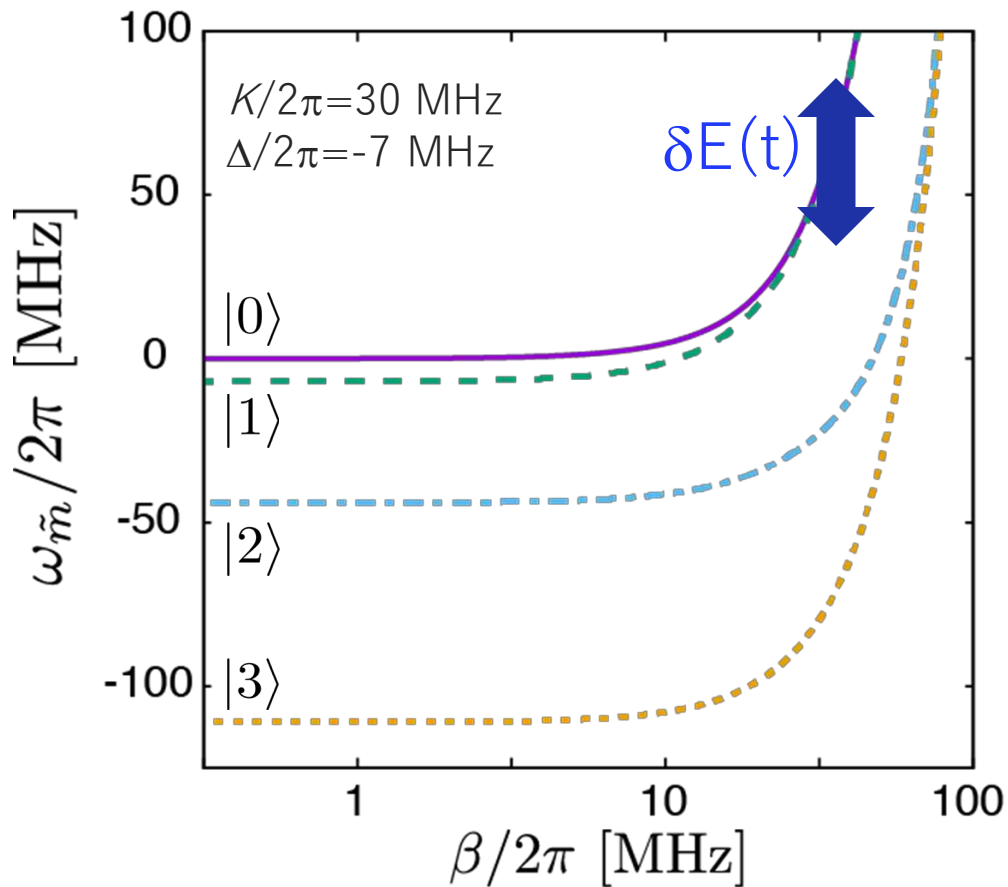
$$H \begin{pmatrix} e^{-i\phi/2} & 0 \\ 0 & e^{i\phi/2} \end{pmatrix} H = \begin{pmatrix} \cos \frac{\phi}{2} & -i \sin \frac{\phi}{2} \\ -i \sin \frac{\phi}{2} & \cos \frac{\phi}{2} \end{pmatrix} = R_x(\phi)$$

R_z gate

H. Goto, Sci. Rep. **6**, 21686 (2016).
S. Puri et al., npj Quantum Info. **3**, 18 (2017).

$$\mathcal{H}_{\text{KPO}}/\hbar = -\frac{K}{2}a^\dagger a^\dagger a a + \beta(a^{\dagger 2} + a^2) + \Delta(t)a^\dagger a$$

detuning $(\omega_0 - \omega_p/2)$



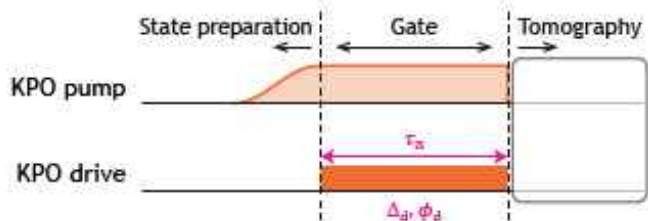
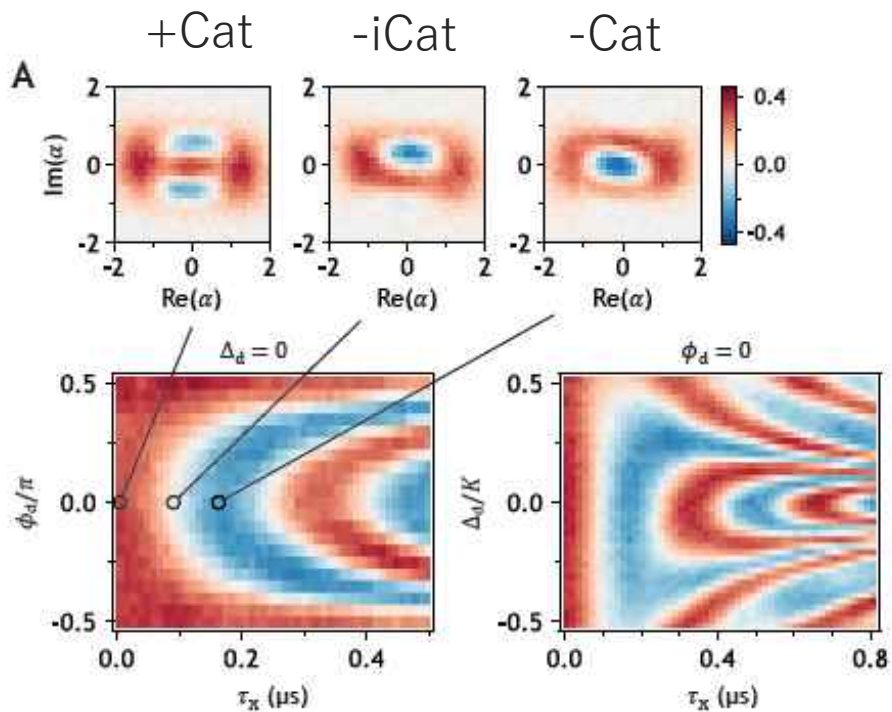
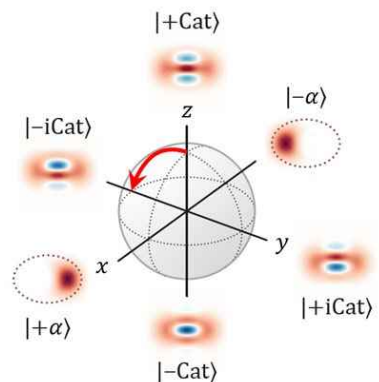
$$\begin{pmatrix} e^{-i\theta/2} & 0 \\ 0 & e^{i\theta/2} \end{pmatrix} \quad \theta = \int_{T_i}^{T_i+T_g} \delta E(t) dt$$

Alternative method:
temporarily remove the two-photon drive. Grim et al., 2020

R_x and R_z gate operations

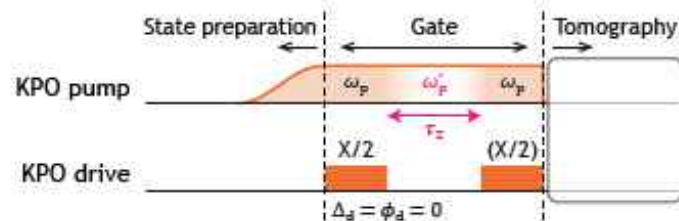
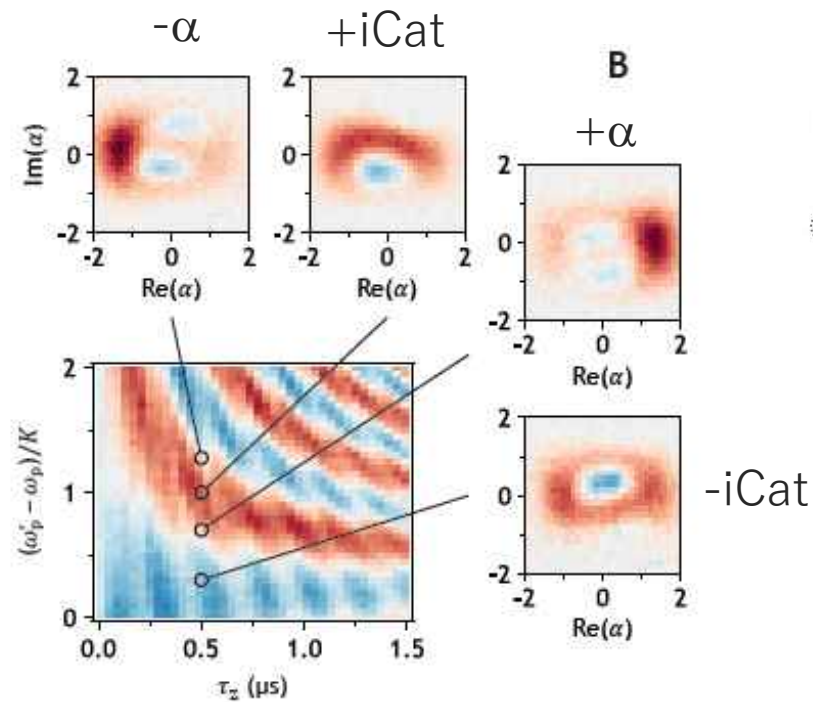
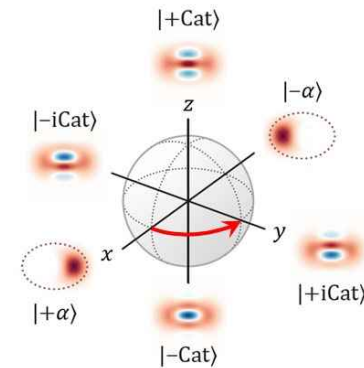
Iyama et al., arXiv:2306.12299.

X rotation



process fidelity for $R_x(\pi/2) = 0.844$

Z rotation

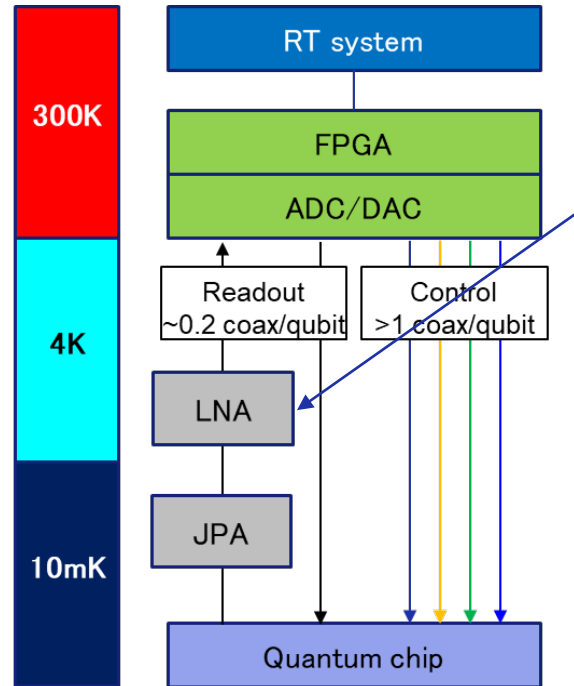


process fidelity for $R_z(\pi/2) = 0.794$

SIS-mixer-based microwave amplifier

Low-noise microwave amplifier for qubit readout

PHYSICAL REVIEW APPLIED 17, 044009 (2022)



Datasheet LNF-LNC4_8F 4-8 GHz Cryogenic Low Noise Amplifier

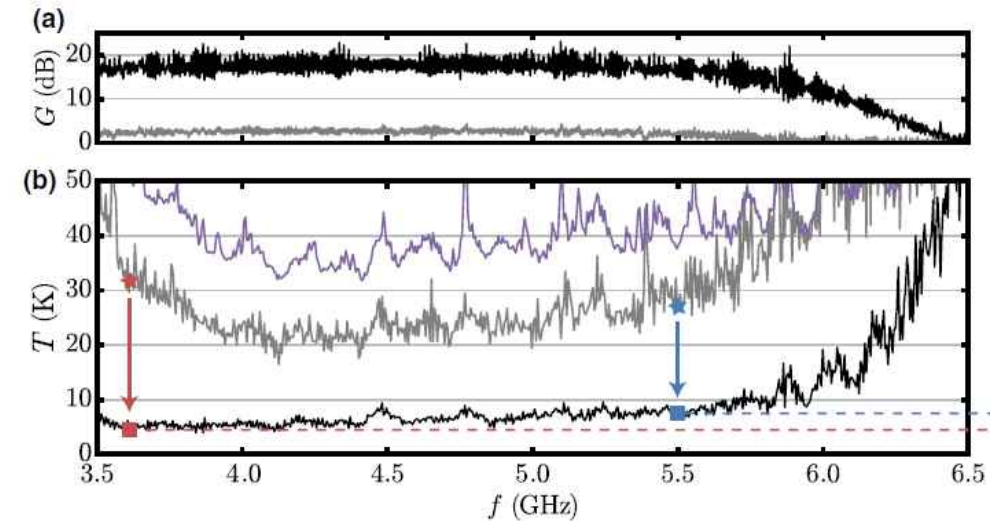
Product Features	
RF Bandwidth	4-8 GHz
Noise Temperature	1.5 K
Noise Figure	0.022 dB
Gain	44 dB
DC power (typical)	$V_{ds} = 0.6 \text{ V}$, $I_{ds} = 13 \text{ mA}^*$
RF Connectors	Female SMA**
DC Connectors	9-pin Female Nano-D
One gate and one drain supply only	



$P \sim 10 \text{ mW}$
 $\sim 1\%$ of cooling power

Performance of a Kinetic Inductance Traveling-Wave Parametric Amplifier at 4 Kelvin: Toward an Alternative to Semiconductor Amplifiers

M. Malnou^{1,2,*}, J. Aumentado,¹ M.R. Vissers,¹ J.D. Wheeler,¹ J. Hubmayr^{1,2}, J.N. Ullom,^{1,2} and J. Gao^{1,2}

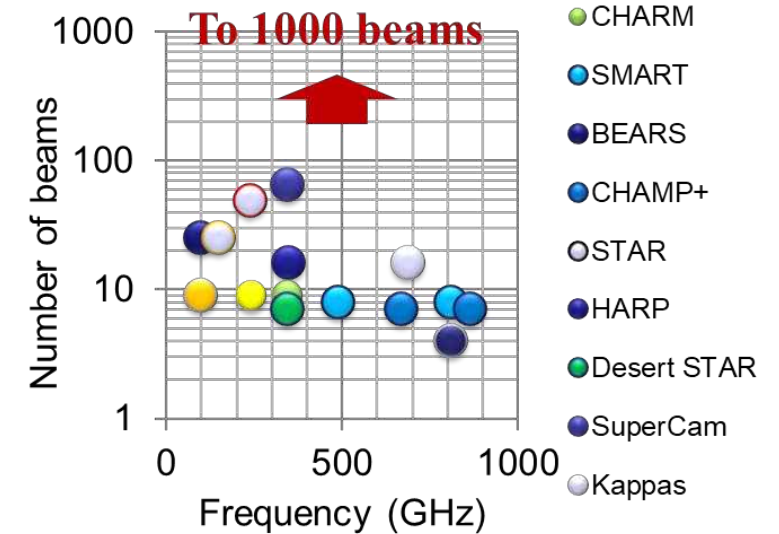
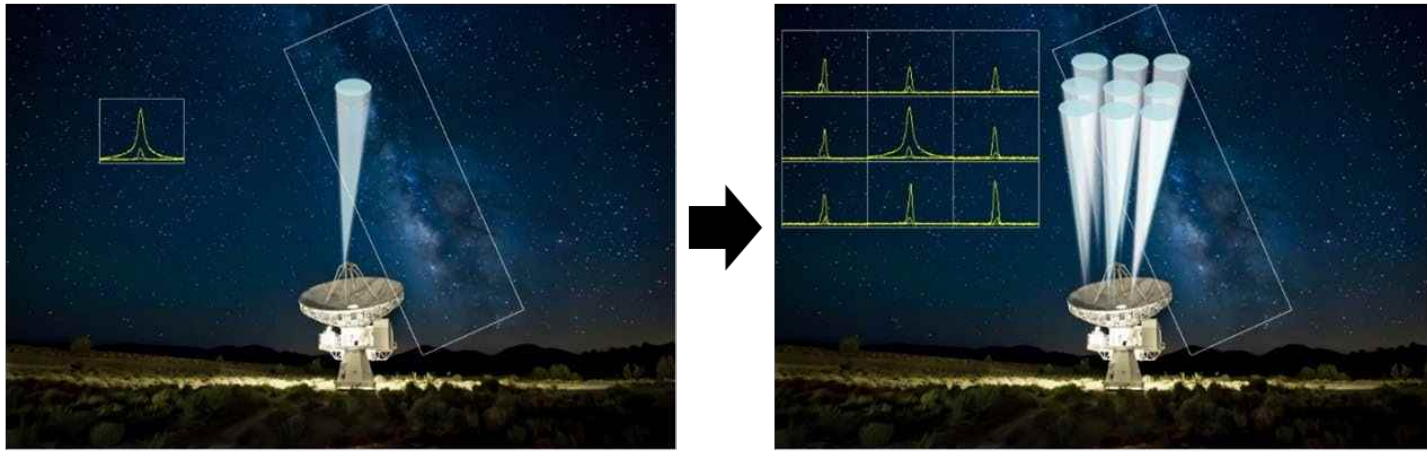


NIST
Gain $\sim 18 \text{ dB}$
Noise temperature $\sim 1.9 \text{ K}$
 $P \sim 100 \text{ uW}$
(RF driven)

Scalability problem in radio astronomy

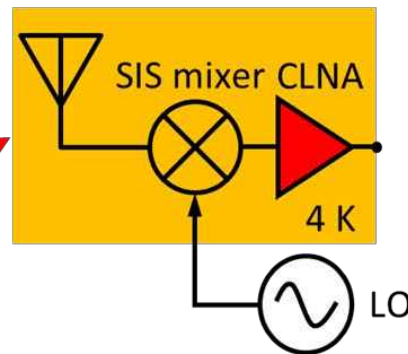
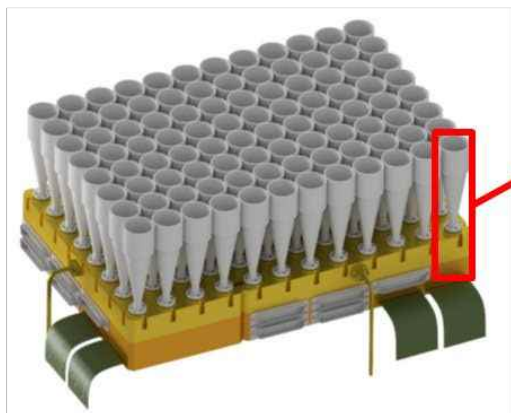
slide courtesy, Y. Uzawa

■ Superconducting receivers in telescopes go from single-beam to multi-beam



Observation efficiency proportional to the number of beams

■ Challenges in scaling up multibeam receivers



Challenge 1

Make compact of receiver frontend
=> integrated superconducting circuit

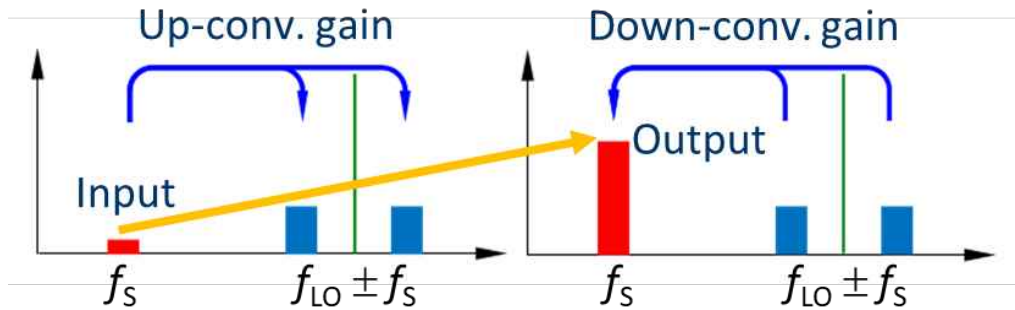
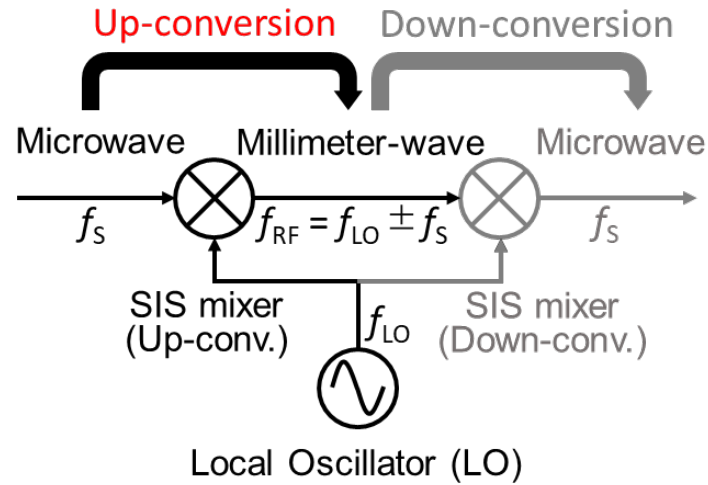
Challenge 2

Reduction of power consumption at the 4K stage
Semiconductor-based amplifier: 10 mW => 10 W (/1000 beams)
=> Low power consumption, low noise, broadband CLNA

SIS-mixer-based microwave amplifier

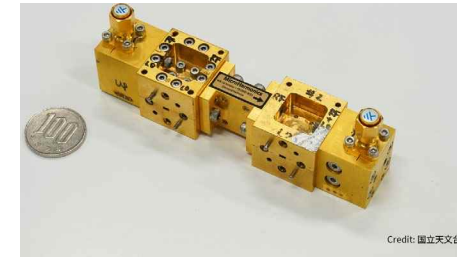
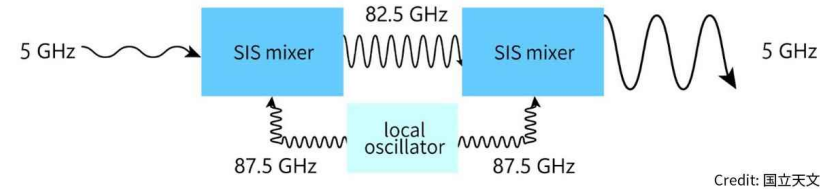


Y. Uzawa



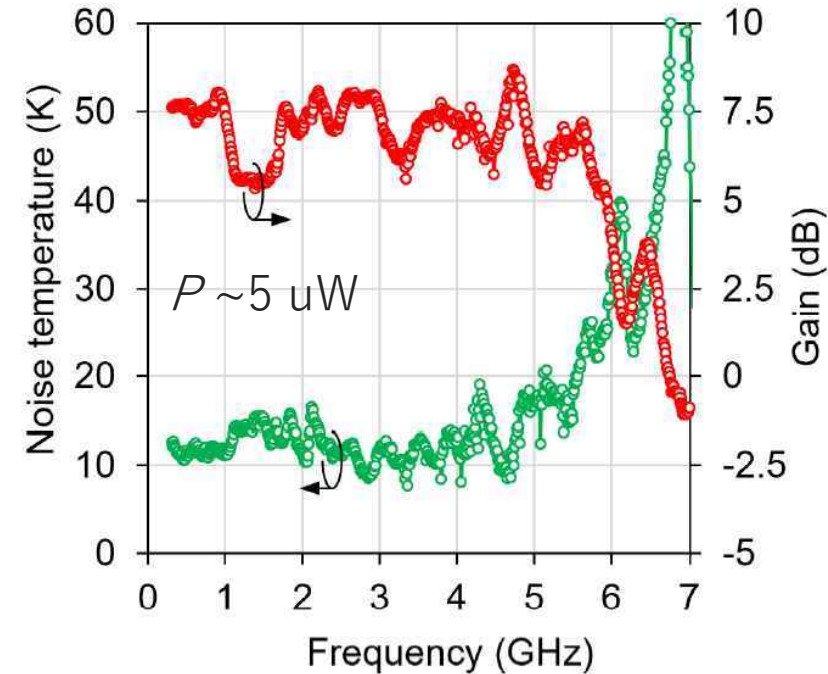
Y. Uzawa et al.,
J. Low Temp. Phys. **193**,
512 (2018).

T.-M. Shen et al.,
Appl. Phys. Lett. **36**,
777 (1980).



Credit: 国立天文台

Credit: 国立天文台

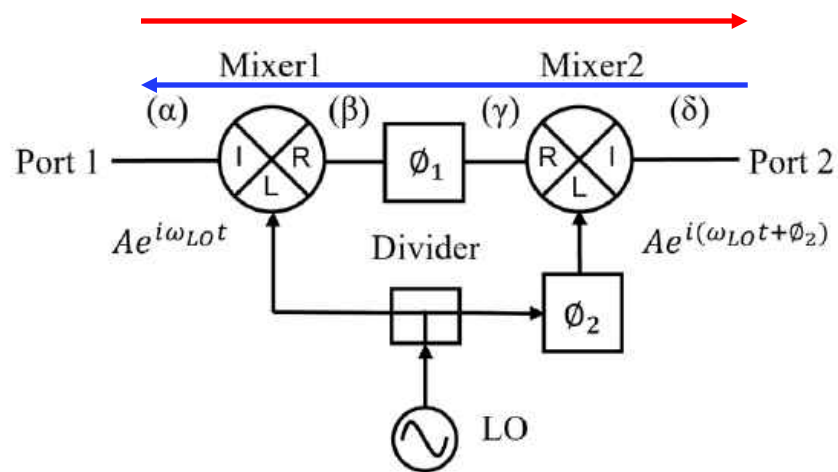


T. Kojima et al.,
Appl. Phys. Lett. **122**, 072601 (2023).

<https://atc.mtk.nao.ac.jp/news/20230320/>

mixer-based non-reciprocity

S. Masui et al., IEEE Microw. Wirel. Technol. Lett. **33**, 1051 (2023).

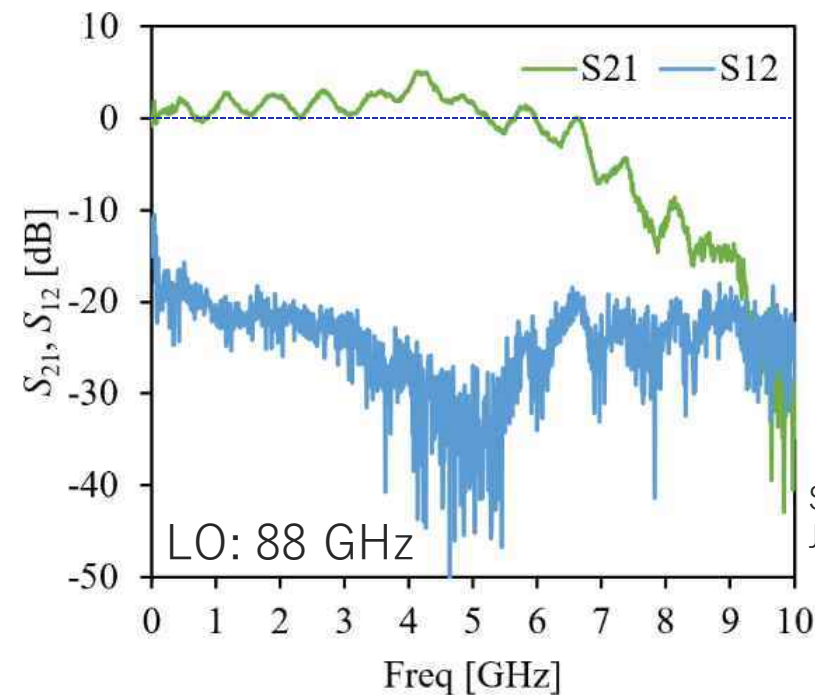
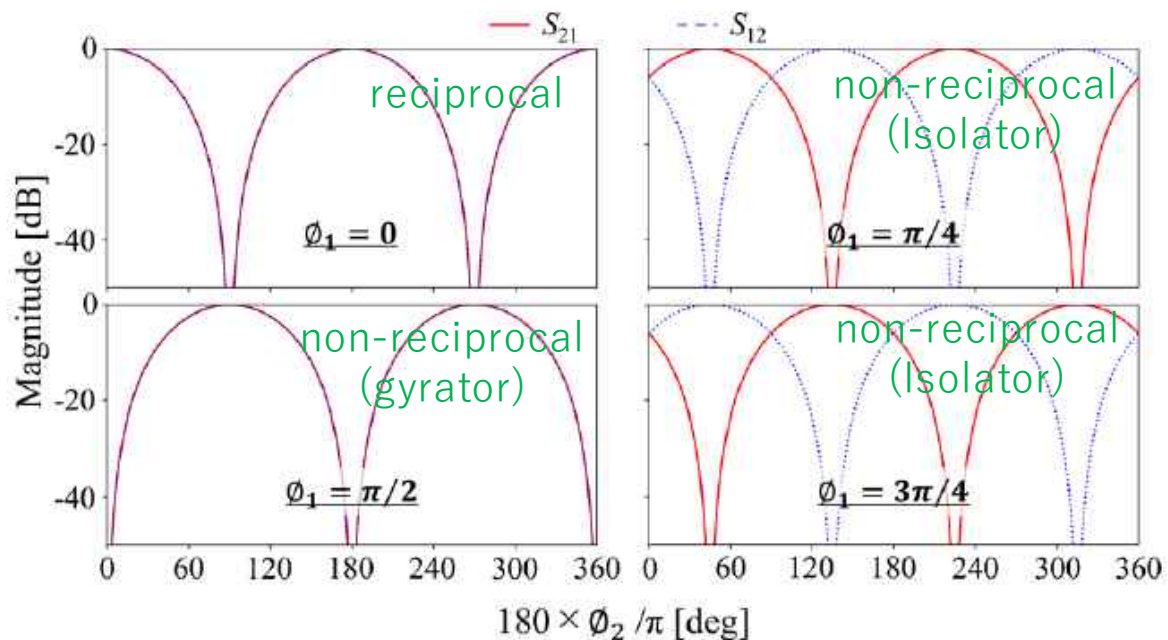


$$S_{21} = G_{\text{USB}} e^{j(\phi_1 - \phi_2)} + G_{\text{LSB}} e^{-j(\phi_1 - \phi_2)}$$

$$S_{12} = G_{\text{USB}} e^{j(\phi_1 + \phi_2)} + G_{\text{LSB}} e^{-j(\phi_1 + \phi_2)}$$

upper sideband

lower sideband



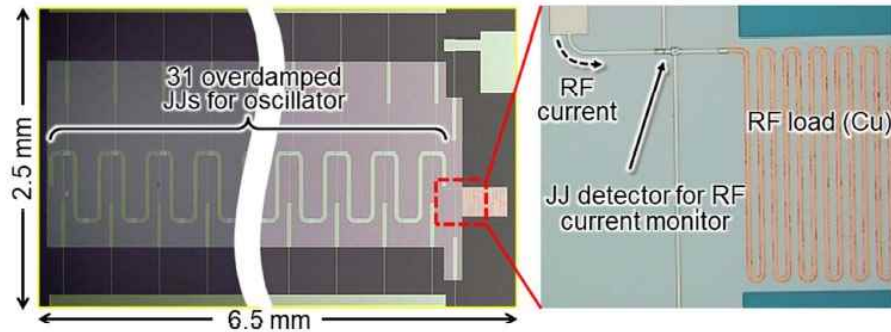
S. Masui et al.,
JSAP meeting 2023 spring

Josephson oscillator for LO source



A. Kawakami

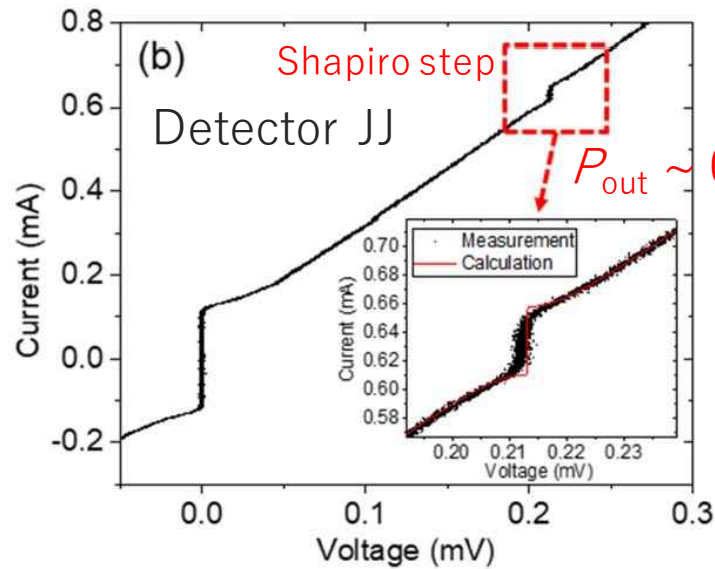
100 GHz Josephson array oscillator with a detector JJ



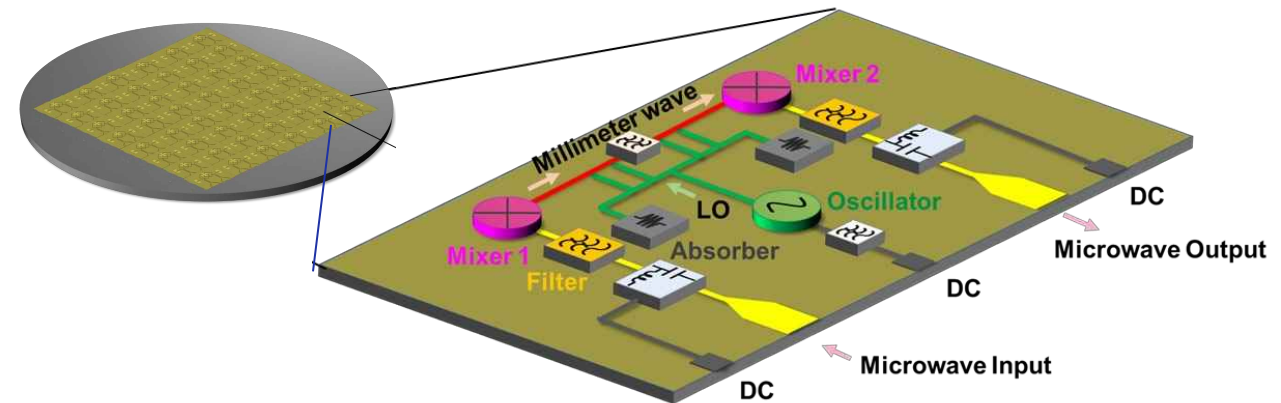
Our goal:

SIS-mixer based amplifier
+
Josephson oscillator

monolithic chip



low power ($\sim \mu\text{W}$)
directional gain
only dc power supply



Y. Uzawa et al., IEEE Trans. Appl. Supercond. **33**, 1500804 (2023).

Plans for the second half of the project

Plans for the second half of the project

Development of cryo-electronics

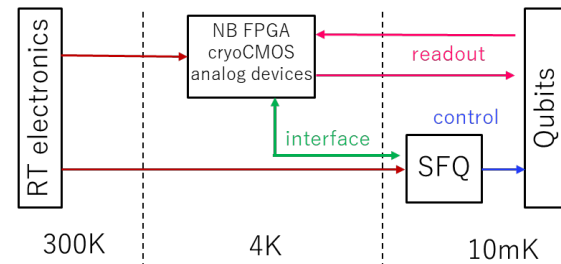
- construction of standard cell libraries
 - ✓ low j_c SFQ circuits for 10 mK operation
 - ✓ digital and analog CMOS circuits for 4 K operation

- operation test of functional circuits
 - test of individual circuits
 - demonstration of qubit control/readout
 - interface between cryo-electronics

System-level architecture exploration

- Develop an evaluation environment of QCP + QCI*
 - e.g. evaluate maximum # of qubits under the constraint of cooling power and required logical error rate for a given hardware configuration
- Evaluate the impact of core technologies developed in the project
- Propose future direction of in-refrigerator system architecture

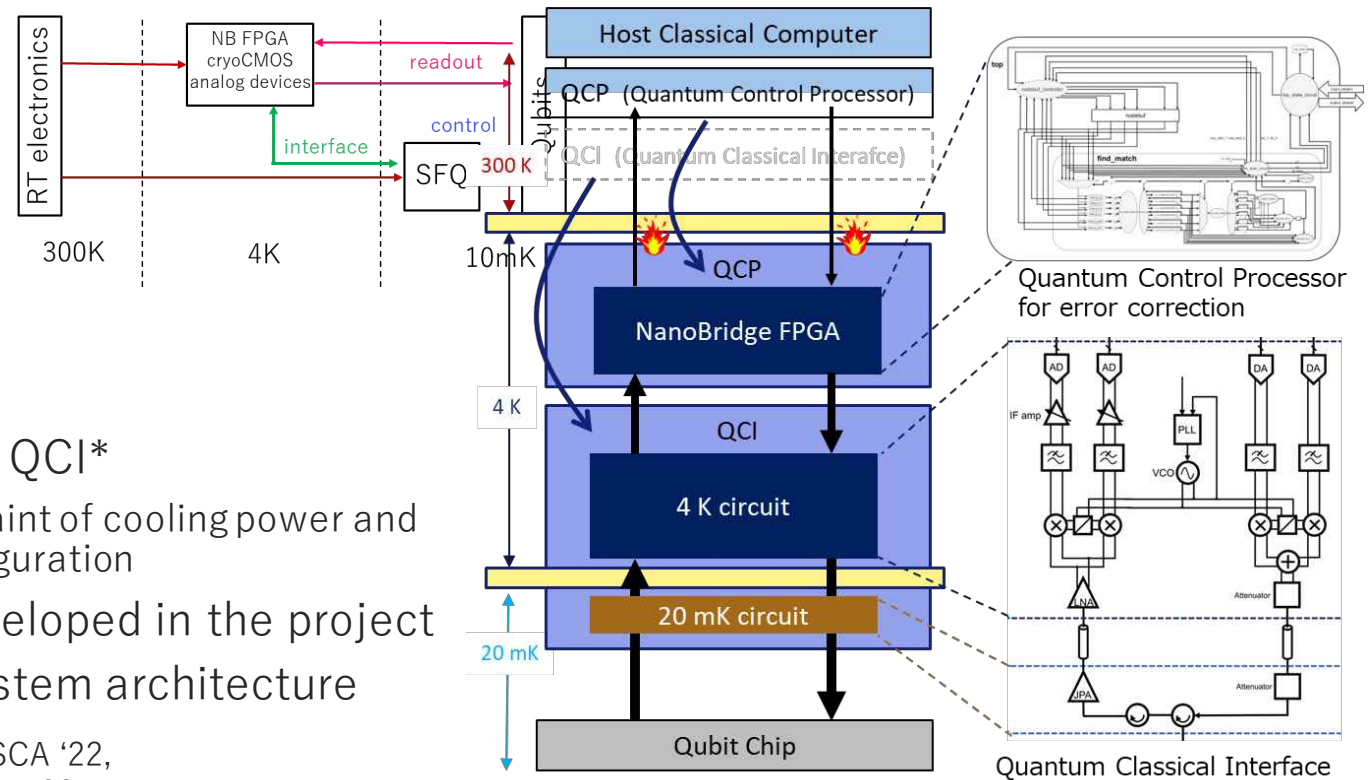
* I. Byun et al., Proceedings of ISCA '22,
D. Min et al., Proceedings of ISCA '23.



K. Inoue



System-Level Architecture Exploration



\Orchestrating a brighter world

NEC creates the social values of safety, security, fairness and efficiency to promote a more sustainable world where everyone has the chance to reach their full potential.

\Orchestrating a brighter world

NEC